



Assessment of potential impact of magnetic fields from a subsea high-voltage DC power cable on migrating green sturgeon, *Acipenser medirostris*

Megan T. Wyman^{1,2} · Robert Kavet³ · Ryan D. Battleson¹ · Thomas V. Agosta¹ · Eric D. Chapman^{1,4} · Paul J. Haverkamp² · Matthew D. Pagel¹ · A. Peter Klimley¹

Received: 15 June 2023 / Accepted: 7 September 2023 / Published online: 16 October 2023

© The Author(s) 2023

Abstract

Empirical evidence suggests that marine animals perceive and orient to local distortions in the earth's natural magnetic field. Magnetic fields (MFs) generated by electrified underwater cables may produce similar local distortions in the earth's main field. Concern exists that these distortions may impact migration movements of MF-sensitive animals. The Trans Bay Cable (TBC) is a ± 200 -kV, 400-megawatt, 85-km high-voltage direct current transmission line buried through San Francisco Bay ($37^{\circ} 56' 8.81''$ N, $122^{\circ} 27' 0.19''$ W). Detections of adult green sturgeon implanted with acoustic transmitters were used from six cross-bay receiver arrays from 2006 to 2015 to investigate how inbound and outbound migration movements through lower portions of their route to/from upstream breeding grounds are related to the TBC's energization status (off/on) and other local environmental variables. Here, we assess how these variables impacted transit success, misdirection from the migration route, transit times, and migration path locations within stretches between the Bay's mouth and the start of the Sacramento River. Overall, there was varied evidence for any effect on migration behavior associated with cable status (off/on). A higher percentage of inbound fish successfully transited after the cable was energized, but this effect was nonsignificant in models including temperature. Outbound fish took longer to transit after cable energization. Inbound and outbound migration path locations were not significantly influenced by cable energization, but results suggest a potential subtle relationship between energization and both inbound and outbound paths. Overall, additional migration-based studies are needed to investigate the impact of anthropogenic cables on marine species.

Keywords Anadromous fish · Animal movement and migration · Biotelemetry · Electromagnetic fields (EMFs) · Subsea power cables · Green sturgeon

Responsible Editor: E. Hunter.

A. Peter Klimley, Robert Kavet: Retired.

✉ Megan T. Wyman
wyman.mt@gmail.com

✉ A. Peter Klimley
apklimley@ucdavis.edu

¹ Biotelemetry Laboratory, Department of Wildlife, Fish, and Conservation Biology, University of California-Davis, Davis, CA, USA

² Department of Evolutionary Biology and Environmental Science, University of Zurich, Zurich, Switzerland

³ Electric Power Research Institute, Environment Sector, Palo Alto, CA, USA

⁴ ICF, Sacramento, CA, USA

Introduction

Subsea electrical power cable utilization is expanding rapidly on a global scale. The development of renewable marine-based energy resources (e.g., offshore wind farms, wave-, current-, or tidal-based power) continues to increase and requires submerged electrical power cables connected to land-based substations, as well as possible inter-array cable connections (Hutchison et al. 2020a). Subsea cables are also increasingly used for a range of other applications such as energy security, interconnecting power grids, and energy transportation across bodies of water or along coastlines. Consequently, there is increasing interest in the potential environmental impacts of these subsea cables, including the effects of electromagnetic field (EMF) emissions (Taormina et al. 2018;

Gill and Desender 2020). Magnetic fields (MFs) penetrate through the water column, while direct electric fields (EFs) can be eliminated through cable shielding. Induced EFs can also be generated by AC cables or when an animal or saltwater moves through these anthropogenic MFs (as well as geomagnetic fields) (Newton et al. 2019). A key concern is whether these anthropogenic sources of EMF may affect the behavior and physiology of EMF-sensitive species with potentially significant effects on migration, foraging, predator avoidance, and reproduction (Tricas and Gill 2011; Gill et al. 2014; Hutchison et al. 2020a; Nyqvist et al. 2020; Klimley et al. 2021). These potential effects could ultimately impact population size and demographics with consequences at an ecosystem-wide level.

Studies demonstrating the effects of EMF perturbations or alterations on the behavior of EMF-sensitive species have been conducted mainly in laboratory or semi-natural mesocosm conditions (Basov 1999; Meyer et al. 2005; Gill et al. 2009; Kimber et al. 2011; O'Connell et al. 2011; Bevelhimer et al. 2013; Anderson et al. 2017) with limited in situ field studies (Westerberg and Lagenfelt 2008; O'Connell and He 2014; Wyman et al. 2018a; Hutchison et al. 2020b). A high priority has been placed on in situ studies investigating the effects of cables on migration behaviors due a paucity of knowledge on this subject (Gill et al. 2012; Klimley et al. 2021). These studies can be especially important given the ecological, cultural, and/or economic value of many migrating species (Klimley et al. 2021).

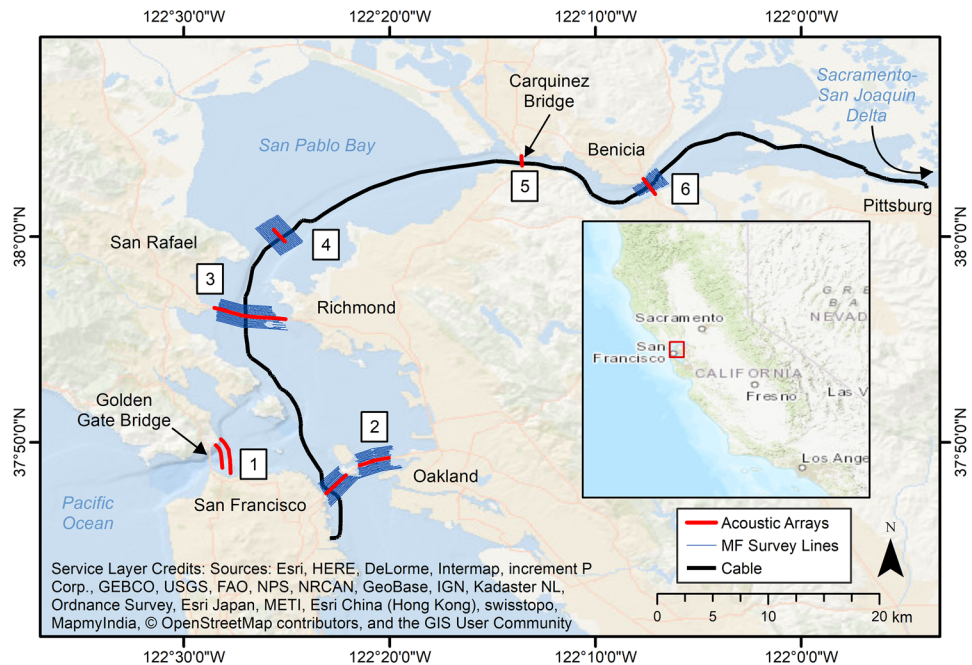
A wide variety of migrating species use geomagnetic cues as a map, compass, or topotaxis guide for orientation or navigation (see reviews Putman 2018; Formicki et al. 2019; Klimley et al. 2021; Lohmann et al. 2022). Detection and response thresholds are species-specific and remain largely untested, but even very small differences in MF intensity, inclination angle, or direction may be detected and used for navigation (Naisbett-Jones et al. 2017; Keller et al. 2021). As such, these migration behaviors may be vulnerable to disruption since a cable's current (also called its "load") can produce local distortions in the earth's natural or geomagnetic field at levels detectable by MF-sensitive species (Tricas and Gill 2011; Hutchison et al. 2021). For instance, species that navigate using local magnetic topography, e.g., scalloped hammerhead sharks that complete daily directional movements to and from feeding grounds along local magnetic maxima ("ridges") and minima ("valleys") (Klimley 1993), could potentially be misdirected by the linear MF perturbations created by cables. Previous in situ studies found that subsea cables had some impacts on the movement behaviors of migrating EMF-sensitive species, e.g., European eels (*Anguilla anguilla*) (Westerberg and Begout-Anras 2000; Westerberg and Lagenfelt 2008) and juvenile late-fall run Chinook salmon (*Oncorhynchus tshawytscha*) (Wyman et al. 2018a), but all suggest further study is required.

Here, we examine the migration behaviors of adult green sturgeon (*Acipenser medirostris*) in relation to subsea cable energization. The subsea high-voltage direct current (HVDC) Trans Bay Cable (TBC) in San Francisco Bay (SF Bay, 37° 56' 8.81" N, 122° 27' 0.19" W) was installed through an important portion of the spawning migration pathway for a key population of green sturgeon. The installation of this cable provided a highly valuable in situ "natural" experiment that allowed the assessment of potential impacts of cable-generated EMF on an essential life phase of this species.

Green sturgeon (GS) are a long-lived (> 40–50 years, Beamesderfer et al. 2007) anadromous species of conservation concern (NMFS 2006) whose family (Acipenseridae) displays both magneto- and electro-reception (Gibbs and Northcutt 2004; Tricas and Carlson 2011; Bevelhimer et al. 2013). Adult GS spend most of their life in the Pacific Ocean, returning to spawn in natal rivers along the west coast of North America every 2–4 years on average (Erickson and Webb 2007; Mora et al. 2018; Miller et al. 2020). The southern Distinct Population Segment (sDPS) of GS enter the SF Bay in late winter and spring and then migrate upstream to spawning sites in the upper Sacramento River and its tributaries (Heublein et al. 2009; Thomas et al. 2014; Seesholtz et al. 2015; Poytress et al. 2015; Wyman et al. 2018b; Steel et al. 2019) before migrating back downstream through the SF Bay to the ocean in either late spring or winter (Colborne et al. 2022). Young sturgeon migrate down to rearing grounds in the Sacramento–San Joaquin Delta and SF Bay Estuary where they remain as juveniles for the next two to three years (Moyle 2002; Thomas et al. 2019) before they begin frequent movements into the Pacific Ocean as subadults (Miller et al. 2020). The sDPS of GS are listed as federally threatened (NMFS 2006), mainly due to human activities (Adams et al. 2007; Heublein et al. 2009; Mora et al. 2009; NMFS 2015), highlighting the importance of examining any potential impacts from anthropogenic EMF. In addition to repeated exposure to the TBC during periodic spawning migrations, their lengthy marine residences and extensive coastal migrations to overwintering regions (Lindley et al. 2008; Miller et al. 2020) place adult GS at further risk of encountering additional subsea cables from marine energy production and transportation or interconnecting power grids (Moser et al. 2016).

The bipolar TBC, ± 200 -kilovolt (kV) with a 400-megawatt (MW) capacity (i.e., up to 1000 amperes (A)), is an 85-km-long interconnector transmission cable that transfers existing power from Pittsburg, CA to San Francisco, CA (Fig. 1). Crucially, the cable route is at times parallel or perpendicular to the GS migration route, depending on the location. Previously, Kavet et al. (2016) described the effect of the TBC's load on the local MF: The cable anomaly deviated from background with a central tendency of ~ 10 nT

Fig. 1 Study map of the San Francisco Bay area. The Trans Bay Cable route (black line) runs from Pittsburg, CA (upper right), to San Francisco, CA (lower left). Fish detecting arrays (red lines) were located at (1) Golden Gate Bridge, (2) Oakland Bay Bridge, (3) Richmond–San Rafael Bridge, (4) San Pablo Bay, (5) Carquinez Bridge, and (6) Benicia–Martinez Bridge. The magnetic field (MF) survey line locations are indicated in blue lines. The lower portion of the migration route of green sturgeon runs between the Sacramento–San Joaquin Delta (upper right) and the mouth of the Pacific Ocean (lower left). [Adapted from Wyman et al. 2018a]



and displayed a wide dispersion, at a distance of approximately 35 m from the cable's location (Wyman et al. 2018a). Theoretically, MF-sensitive species can detect MF anomalies < 10 nT (Tricas and Gill 2011). Although thresholds of EMF perception in GS are unknown, previous laboratory studies have observed that juvenile lake sturgeon (*Acipenser fulvescens*) alter swimming behaviors in response to MFs above a threshold level of 1000–2000 μ T (Bevelhimer et al. 2013). Also, other sturgeon species alter their behaviors in response to experimental changes in EFs (Russian sturgeon, *Acipenser gueldenstaedtii*, and sterlet, *Acipenser ruthenus*, Basov 1999; lake sturgeon, Stoot et al. 2018). In a previous study, Wyman et al. (2018a) assessed the effect of the TBC on juvenile late-fall run Chinook salmon outmigration behaviors in the same area and found that cable energization was associated with reduced transit duration and altered movement paths through some regions but did not influence migration success (i.e., ability to exit the SF Bay).

Prior to the time the TBC was installed, GS migration patterns were already under study using acoustic telemetry within the SF Bay watershed (Kelly et al. 2007; Heublein et al. 2009; Thomas et al. 2014). Thus, by comparing movement patterns and migration success during periods when the cable was not energized vs. energized, we can investigate if the presence of the energized cable (and by inference, its MF) affected migratory behavior. While we acknowledge that induced EFs from subsea cables may also play an important role in electrosensitive sturgeon responses (Newton et al. 2019; Nyqvist et al. 2020), here we focus on the potential influence of cable MF anomalies on migration behaviors due to wide evidence for the use of MFs

in migration-related navigation and orientation behaviors across many species (see reviews Putman 2018; Klimley et al. 2021; Lohmann et al. 2022).

We used detections of adult GS implanted with uniquely coded acoustic transmitters at six cross-bay arrays of receivers to investigate how the inbound and outbound migration movements to/from the upstream breeding grounds are related to variables associated with the TBC and local environmental factors. Here, we assess the relationship of these variables to transit success, misdirection from the migration route, transit times, and the locations of migration paths through the lower portion of their migration route to/from upstream breeding grounds.

Materials and methods

Study location

The HVDC TBC originates at the city of Pittsburg, CA, located at the edge of the SF Bay Delta, a network of sloughs and channels (Fig. 1). The cable runs along the south side of the main channels of Suisun and San Pablo Bays, crosses the deep flat bottom of SF Bay, and comes ashore in San Francisco at the Potrero substation, south of the mouth of the estuary and the Oakland Bay Bridge. This bipolar cable, consisting of two conductors separated by 0.1143 m and covered with a conductive sheath to shield EFs, is buried approximately 2 m under the channel bottom (Kavet et al. 2016). The cable was activated in 2010 with the capacity to

provide a significant portion (up to 40%) of San Francisco's power needs.

Adult GS used in this study were captured and tagged with uniquely coded ultrasonic 69-kHz transmitters (V16, Innovasea Systems Inc. (formally VEMCO, Inc.), Boston, USA). Tagged fish were detected on submersible acoustic receivers (VR-02 and VR-02w, Innovasea Systems Inc.) attached to bridges or anchored on the channel bottom within SF Bay. These receivers were arranged in cross-channel linear arrays along five bridges and one open area (Fig. 1): (1) Golden Gate Bridge arrays (9–23 receivers, 0.8–1.7 river-km, rkm, with 0 rkm occurring directly upstream of the Golden Gate Bridge), (2) Oakland Bay Bridge array (Bay Bridge, 9–22 receivers, 10.0–13.2 rkm), (3) Richmond–San Rafael Bridge array (Richmond Bridge, 15–35 receivers, 14.7 rkm), (4) San Pablo Bay array (8 receivers, 22.3 rkm), (5) Carquinez Bridge array (8 receivers, 41.5 rkm), and (6) Benicia–Martinez Bridge array (Benicia Bridge, 7 receivers, 51.7 rkm). Additional non-array receivers located at Pt. Reyes (north of the mouth of SF Bay) and other locations upstream from Benicia Bridge were also used to help classify migration movements. All receivers used in this study were part of a larger passive acoustic monitoring network placed throughout the SF Bay Estuary, Sacramento–San Joaquin Delta, and Sacramento River (maintained primarily by the Biotelemetry Laboratory at the University of California, Davis, and the National Oceanic and Atmospheric Administration; see <https://cftc.metro.ucdavis.edu/default.shtml>).

During a typical inbound breeding migration, GS would pass from the Pacific Ocean through the Golden Gate, then turn north to pass through Richmond Bridge and eastward through the southern portion of San Pablo Bay (where the array was located), and then enter the narrow Carquinez Straight between Carquinez Bridge and Benicia Bridge toward the southwestern section of the Sacramento–San Joaquin Delta before turning northwards to the upper Sacramento River and its tributaries to spawn. A typical outbound migration route would be the reverse.

Green sturgeon detections

This study incorporates detections of fish from previous acoustic telemetry studies carried out on GS both before and after the TBC was installed through SF Bay. Adult GS used in this study were tagged by intracoelomic surgical implantation of uniquely coded ultrasonic transmitters (V16-6, Innovasea Systems Inc.). Capture and tagging occurred between 2005 and 2014, mostly within northern California (Sacramento River and tributaries, Sacramento–San Joaquin Delta, and SF Bay; see Thomas et al. 2014 for an example of tagging procedures) as well as some locations in Oregon and Washington (Umpqua River, Columbia River, Chehalis

River, and Willapa Bay). Tagging was carried out in previous research by University of California, Davis, National Marine Fisheries Service, US Bureau of Reclamation, California Department of Water Resources, Oregon Department of Fish and Wildlife, Washington Department of Fish and Wildlife, and Natural Resource Scientists, Inc. Transmitters for these studies produced uniquely coded pulses at random delays ranging between a minimum of 37 s and a maximum of 180 s, depending on the study, and had a 10-year battery life. Range tests were conducted to estimate the distance at which these transmitters could be detected by the receivers within the study location. Drift range tests were conducted at the Richmond Bridge hydrophone array (a geographical midpoint of the study area) using an ultrasonic V16-6L transmitter (69 kHz, 152 dB re: 1 μ P @ 1 m, fixed pulse rate: 20 s, Innovasea Systems Inc.), similar in size and power to the range of transmitters used in the detection data for this study, attached to a weight and submerged 1.5 m below a buoy float equipped with a GPS unit (GPSMAP 78sc, Garmin Ltd., USA). During three outgoing tides and two incoming tides, the buoy was released near the center of the channel approximately 1 km from Richmond Bridge and allowed to passively float past the bridge's array. GPS locations of the buoy and detection records of the drifting transmitter at the bridge array receivers were used to calculate the detection range, defined here as the maximum distance at which at least 75% of the coded acoustic pulses emitted by the test transmitter were detected by receivers. This distance was calculated to be 230 m.

Detections from a total of 238 adult GS occurring between October 2006 and March 2015 comprised the initial dataset. Only reproductively mature adult GS were included in this analysis, defined as fish with a fork length of at least 1390 mm (Van Eenennaam et al. 2006). Since no fish with recorded fork lengths below the threshold of 1390 mm were detected in the spawning grounds of the upper Sacramento River (> 400 rkm), GS without recorded lengths were also counted as reproductively mature adults if they were detected in the Sacramento River above 400 rkm and were tagged with V16 tags (as opposed to smaller Innovasea Systems Inc. V9 or V13 tags used in younger fish).

Exclusion criteria were applied to this initial dataset in order to maximize data quality and to correctly classify migration types. Detections per individual were not used if they were as follows: (1) within 30 days of tagging to eliminate capture and handling effects, (2) only present at one location (as probable migration direction could not be characterized; see below), or (3) < 5 total detections per individual in the system (from Sacramento River through the SF Bay). The capture and handling associated with tagging can potentially disrupt migration behaviors, as documented in GS and other sturgeon species (see Benson et al. 2007; Erickson and Webb 2007). Our 30 days post-tagging

limitation (consistent with Miller et al. 2020) was implemented as a wide precaution against these effects. Our threshold of at least five total detections was established to prevent the use of potentially atypical fish or tags (e.g., faulty transmitters) with an abnormally low number of detections (i.e., their movements and migration direction may be poorly characterized or non-representative of the population). Furthermore, we did not include any detections that occurred between January 1 and November 23, 2010, as load data for the TBC during this operational testing period were unknown. The average daily load data (MW) carried by the TBC from the official activation date of November 23, 2010 onward were provided by Trans Bay Cable LLC (Table 1).

While the GS spawning migration route stretches from the mouth of the SF Bay at the Pacific Ocean to > 400 rkm upstream of the Golden Gate Bridge along the Sacramento River and its tributaries (Miller et al. 2020), this study only examined GS movements within the lower portion of this route, between the mouth of the SF Bay to near the start of the Sacramento River just upstream of its confluence with the San Joaquin River (hereafter “lower migration route”). The TBC is present from ~7 rkm from the mouth of the Golden Gate Bridge to ~75 rkm where it connects to land in Pittsburg (Fig. 1). Classification of inbound sturgeon migration movements required the fish to be first detected at the start of the migration at the outer edge of SF Bay (Pt. Reyes or Golden Gate Bridge receivers) between January and June, as is typical for reproductive migrations (Heublein et al. 2009). An inbound movement was defined as a successful migration transit through the lower migration route if the fish was subsequently detected > 85 rkm upstream of the Golden Gate Bridge (near the start of the Sacramento River as it splits from the Sacramento–San Joaquin Delta, indicating that it traveled through the SF Bay, past the TBC, and into the start of the Sacramento River) and unsuccessful (i.e., an “aborted” inbound transit) if the fish was not detected > 85 rkm. Acoustic receivers upstream of this 85 rkm limit started near Decker Island at 86.3 rkm. Outbound adult sturgeon migrations, which can occur during any season (Miller et al. 2020) with two main peaks in May–June and November–January (Colborne et al. 2022), were defined by the detection of fish > 85 rkm before being detected in SF Bay. An outbound transit was defined as successful if the fish was detected at Golden Gate Bridge or Pt. Reyes after traveling through the SF Bay and unsuccessful (i.e., an “aborted” outbound transit) if they were not.

Binary migration descriptors (yes or no data) were assigned to each fish’s migration movements, with the following outcome variables:

- *Successful Transit* indicated if the inbound or outbound fish passed completely through the lower migration route.

Here, “success” simply implies that the fish made a full transit through the lower migration route based on available detection data.

- *Misdirected* indicated a fish that was detected at a Bay Bridge receiver, because the Bay Bridge is south of the migration path in and out of the bay. Since the Bay Bridge receivers were not operational until February 10, 2007, analyses that included this variable were restricted to detections occurring after this date.

For each fish, transit times for inbound and outbound migrations were calculated within specific reaches, i.e., segments of the migration pathway between specific bridges, defined as the total amount of time between the last detection at an array on one edge of a reach and the first detection at the subsequent array at the opposite end of that reach. Transit times were calculated within three reaches: outer reach between Richmond Bridge and Golden Gate Bridge; inner reach between Carquinez Bridge and Richmond Bridge; and total reach as the total distance between the Carquinez Bridge and Golden Gate Bridge (Fig. 1). Carquinez was used as a reach border for sturgeon instead of Benicia, as used in our previous study of Chinook salmon (Wyman et al. 2018a), because the arrays were installed earlier at Carquinez than at Benicia, thus allowing inclusion of more detection records.

Lengths of the sturgeon were not included in any statistical models in this study because these measurements were not available for all fish both prior to and after the TBC was energized, and omissions could cause biased results. Furthermore, differences between tagging date, detection dates, and the exact age of fish at tagging meant that accurate lengths could not be assigned to each detection across time.

Characterization of magnetic fields

Magnetic field surveys were conducted at four locations in the SF Bay between July 10 and August 8, 2014. MF values were measured using a gradiometer composed of twin cesium magnetometers separated by 1.5 m (G-882 TVG, Geometrics, Inc., San Jose, CA), towed from a research vessel. The surveyed areas overlapped with acoustic telemetry arrays situated along the Benicia–Martinez Bridge, the Richmond–San Rafael Bridge, and the Oakland Bay Bridge, along with a non-bridge location in San Pablo Bay (Fig. 1). Survey lines were separated by 100 m and orientated perpendicular to the TBC and parallel to the fish detecting arrays. Surveys were conducted both at the surface (0.5–3 m beneath the water’s surface) and at depth (< 10 m above the channel bottom). Channel depth at the cable location was approximately 13 m at all fish array locations (except Bay Bridge where depth reached 24 m). The overall process of data collection and subsequent transformation into MF maps is shown in Fig. ESM 1. Data from these surveys included

Table 1 Environmental variables associated with fish transits

Variable	Description	Source
Cable energization status (off/on)	Binary descriptor of cable energization status (off/on) per day based on mean daily load data carried by the TBC	Provided by Trans Bay Cable LLC
Net magnetic field (nT): surface and deep	Total magnetic field minus earth's magnetic field, as measured during surface and deep tows. Measures were averaged over the detection range of each receiver, and the absolute value of this average was used in statistical models	Quantified using magnetic field surveys (see text, Fig. ESM 1, Kavet et al. (2016), Klimley et al. (2017), and Wyman et al. (2018a) for additional details). Net magnetic field data were interpolated in MagPick (Tchernychev 2013) on a 2 × 2 m grid and exported to ArcMap (ESRI). In ArcMap, point data were converted to an interpolated raster with 3 × 3 m pixels using the inverse distance weighting tool in 3D Analyst, and net magnetic field values were averaged over each receiver's detection range (230 m)
Magnetic field gradient (nT m ⁻¹): surface and deep	Rate of magnetic field change, as measured during surface and deep tows. Measures were averaged over the detection range of each receiver	Same process as net magnetic field data (above) but for magnetic field gradient measures
Receiver distance to the cable location (km)	Shortest horizontal distance between each receiver and the cable location, regardless of whether the cable has been installed or not; i.e., location represents the eventual or actual location of the cable	Cable route provided as an ArcMap shapefile by Trans Bay Cable LLC. Horizontal distances between receivers and cable measured in ArcMap
Channel depth (m)	Water depth (vertical distance between water surface and channel bottom) as derived from a digital elevation model (DEM) of the SF Bay area. Measures were averaged over the detection range of each receiver	DEM sourced from the National Oceanic and Atmospheric Administration (NOAA) National Geophysical Data Center: SF Bay, California, created in 2010, 1/3 arc-s (~ 10 m) cell size, NAVD 88 Coastal DEM. Data accessed in 2016 from NOAA National Centers for Environmental Information (https://www.ncei.noaa.gov/). Average depth within each receiver's detection range (230 m) was calculated in ArcMap
Time of day (day/night)	Binary descriptor (day/night) for the time of day of each fish detection based on the sunset and sunrise times at each detection date and receiver location	Sunrise and sunset times per detection date were calculated for each receiver location using the <code>sunrise.set</code> function in the R package <code>StreamMetabolism</code> (Sefick 2016)
Temperature (°C)	Daily water temperature averages of hourly readings from the Port Chicago environmental station	Port Chicago station (NOAA station ID: 9,415,144) is approximately 7.5 rkm upstream from Benicia Bridge, near the transition between the Sacramento–San Joaquin Delta and the SF Bay. Data accessed in 2016 through the California Data Exchange Center (https://cdec.water.ca.gov/)
Delta outflow discharge (m ³ s ⁻¹)	Daily water discharge readings from the Delta Outflow environmental station	Delta Outflow station (California Dept. of Water Resources station ID: DTO) is approximately 9 rkm upstream from Benicia Bridge, near the transition between the Sacramento–San Joaquin Delta and the SF Bay. Data accessed in 2016 through the California Data Exchange Center (https://cdec.water.ca.gov/)
Tidal current strength and direction (in_strong, out_weak)	Descriptor of tidal current velocity and direction for each detection. Detections were assigned one of four tidal current descriptors based on current strength (strong: > 1.0 m s ⁻¹ , weak: < 1.0 m s ⁻¹) and direction (inbound, outbound) at the time, date, and array location	Predicted current velocity and direction data at the time and date of max and slack tides were obtained from NOAA weather stations closest to each detection array (~ 0.9–2.7 km from array centers). Data accessed in 2017 via request from the Current Prediction section of the NOAA Tides and Currents webpage (https://tidesandcurrents.noaa.gov/)

These data were quantified at the location of the array receivers and/or assigned based on the date, time, and location of fish detections at the array receivers

the net MF, defined here as a scalar quantity equal to the total MF minus the geomagnetic field, and MF gradient (the latter meaning the rate of change of the absolute net MF with respect to distance, expressed in nT m^{-1}) (Table 1). For further details, see Kavet et al. (2016), Klimley et al. (2017), and Wyman et al. (2018a) where *net* MF is labeled as either *local* or *total* MF, but all refer to the same data definition. See Kavet et al. (2016) for a characterization of MFs from the TBC, highlighting a tight correlation between measured and modeled net MFs, and a comparison of currents derived from measurement profiles to load data provided by Trans Bay Cable LLC.

Environmental variables

In addition to the MF landscape, other environmental factors varied both spatially and temporally along the path of fish migration through the SF Bay. Thus, accounting for them at the time and location of fish detections—along with the cable's status as energized or not (off/on)—was necessary to assess any potential confounding factors affecting the association between the presence of the energized cable and GS migratory behavior (as well as determining potential stand-alone effects). The collection of environmental variables is described in detail in previous publications (Klimley et al. 2017; Wyman et al. 2018a). In addition to the net MF and MF gradient, key environmental variables included the energized status of the cable (off/on), receiver distance to the cable location (km), channel depth (m), time of day (as binary day/night descriptor), temperature ($^{\circ}\text{C}$), delta outflow discharges ($\text{m}^3 \text{s}^{-1}$), and tidal current strength and direction (four categorical descriptors). All environmental variables and sources are described in Table 1. Using ArcMap (ESRI), channel depth and MF values for each receiver were quantified as the average value within the receiver detection range for V16-6L Innovasea Systems Inc. transmitters (calculated as 230 m; see range test description above).

Statistical analyses

Transit success and misdirection

Fisher's exact tests were used to determine if the probability of fish successfully transiting through the lower migration route differed: (1) when the cable was not energized vs. energized (i.e., cable status off/on) and (2) for fish that were detected at the Bay Bridge during their transit, compared to those that were not misdirected (i.e., misdirect no/yes), and (3) to determine if the probability of misdirection differed between pre- and post-cable energization. To reduce pseudo-replication and meet the assumption of independence, repeated observations of fish within either inbound or outbound transits (assessed separately) were removed to

create datasets containing only one observation per fish (i.e., unique fish identity (ID) datasets) representing the first time each fish was observed during these two transit directions.

Expanded environmental models using logistic regression were developed to address which variables influence the inbound and outbound probabilities of the following: (1) fish successfully transiting through the lower migration route (no/yes) and (2) fish detected at the Bay Bridge (no/yes). The main fixed effects for these models included cable energized (off/on), river discharge, and temperature. Detection at the Bay Bridge (no/yes) was also included as a fixed effect in the models examining successful transits. River discharge and temperature values were calculated as the average of daily readings over the median total transit duration of all fish through SF Bay during inbound or outbound transits (between Golden Gate Bridge and Carquinez Bridge or Benicia Bridge, with median duration calculated separately for each direction and rounded up to the nearest number of total days). For inbound fish, daily discharge and temperature readings were averaged over 3 days (rounded up to the nearest day from a median total transit time of 55.5 h) from the last day detected at Golden Gate Bridge, and for each outbound fish, readings were averaged over 2 days (rounded up from a median total transit time of 46.2 h) starting from the last day of detection at Carquinez Bridge or Benicia Bridge. Discharge values were log-transformed to better fit model assumptions. Datasets with unique fish IDs (first observation of each fish) were used in these logistic regressions because using the full dataset with repeated observations per fish and including fish ID as a random effect (i.e., logistic mixed-effects regression models) produced singularity and convergence issues.

For the logistic regressions, a multimodel inference approach employed model averaging of a top set of candidate models instead of selecting a single "best fit" model. This is a common methodological tool in ecological studies to address model uncertainty and provide a more robust assessment of the relationships between the response variable and predictor variables (Burnham and Anderson 2002; Grueber et al. 2011; Dormann et al. 2018). Numeric predictor variables (temperature and discharge) were standardized (mean-centered and divided by two standard deviations, Gelman 2008). All possible models from the null model (intercept only) to the full model (all predictors included) were generated and ordered based on AICc values. A top set of models was identified as those with AICc values less than two ($\Delta\text{AICc} < 2$) from the best fitting model (i.e., the model with the lowest AICc). Using the natural average method, parameter estimates for each predictor were calculated by averaging parameter estimates over each top model that contains that predictor and weighting the estimate by the summed weights of these models (Burnham and Anderson 2002; Grueber et al. 2011).

Transit time

Wilcoxon rank sum tests were used to determine if inbound and outbound transit times through the outer, inner, and total reaches differed significantly (1) when the cable was not energized vs. energized (off/on) and (2) when fish were detected at the Bay Bridge as compared to migrations in which they were not. The Bay Bridge array was not active over the entire study period, and the Bay Bridge data apply to only the outer and total reaches. Unique fish ID datasets were used for these analyses to avoid pseudo-replication and to meet the assumption of independence. Effect size was calculated as the z statistic divided by the square root of the sample size and 95% confidence intervals of the effect size were generated by bootstrap resampling using 10,000 repetitions.

We also examined if additional environmental variables influenced the duration of inbound and outbound transits using linear mixed-effects (LME) models with maximum likelihood estimates. Separate models were developed per reach and transit direction. Fixed effects included cable status (off/on), river discharge, and temperature. Detection at the Bay Bridge (no/yes) was also included for LME models of transit times through the outer and total reach. For the LME analyses, we utilized a dataset that included repeat transits for some fish, and therefore, fish identity was included as a random effect (intercept). River discharge and temperature were averaged over the transit time of each fish through each reach. Transit times and discharge were log-transformed to meet model assumptions. Final model selection involved the multimodel inference approach with model averaging, as described above.

To determine the potential role of outliers, LME models were also run with trimmed datasets that removed extreme outliers (logged transit time values beyond 3 times the interquartile range) per reach and transit direction. Nonetheless, a strong rationale needs to be provided to use the trimmed data in preference to the full dataset.

Location of first detection at arrays

The location of fish migration paths, defined as the position of each fish along each linear receiver array, was assessed using the first detection of fish at the Richmond Bridge, Benicia Bridge, and San Pablo Bay arrays. These single detection points per array provide a “snapshot” of the migration path of each inbound or outbound fish as they approach the cross-channel bridges and open bay area. Two methods addressed which environmental variables were associated with the location of first detection: (1) resource selection functions (a method to analyze which environmental variables account for observed behaviors) using fixed effect conditional logistic regression (CLR)

models (i.e., a matched case–control analysis) and (2) LME regression models focused on variables that predicted the distance of migration paths (i.e., the horizontal position of the fish at the array) from the location of the cable, including both when the cable was energized and not energized.

Firstly, we used CLR models to determine the probability of fish detection based on the environmental parameters present at that location and time at each array. For each array, the first detection records of each fish were organized into matched case–control strata with one stratum per fish per transit and cluster set to fish ID. Within each stratum, the first receiver to detect a fish was designated as the case (detection = 1) and all other receivers in that array were the controls (detection = 0). The response variable of the CLR models was the binary detection factor, representing either a 1 (case) or 0 (controls). At each receiver location, the main fixed effects included distance to cable location, average channel depth, and average net MFs and MF gradients at both surface and deep tows (Table 1, with averages calculated over the detection range of 230 m). The absolute value of the net MF averages was used to represent direction-free local distortions, including those associated with the cable and any other sources. These values were square-root-transformed to better accommodate model assumptions. Additionally, to determine the effects of environmental variables that differ across time but not across array locations (i.e., cable status, discharge, tidal current), such parameters were added as interaction terms with main effect variables, but not as main effects themselves (Fortin et al. 2009). Cable status (off/on) was entered as an interaction with distance to cable location: A significant interaction would indicate that the relationship between fish location and distance to cable location changes as a function of cable status. Similarly, river discharge and tidal current descriptors (values based on the time of first detection at each array) were included as separate interaction terms with channel depth. The best fit CLR model per array was determined for each transit direction (inbound or outbound fish) using stepwise backward selection and defined as the most parsimonious model $< 2 \Delta AICc$ from the minAICc. Global Wald tests determined if the best fit model significantly differed from the null model. Due to positive pairwise correlations among MF measures within some arrays, only surface net MF was included at Richmond Bridge (Spearman rank correlation, $r_s = 0.43$ to 0.83 , $P = 0.008$ to < 0.001), and only surface net MF and surface MF gradient were used at San Pablo Bay (Spearman rank correlation, $r_s = 0.83$ to 0.98 , $P = 0.015$ to < 0.0001). Due to a strong negative correlation between distance to cable location and depth at San Pablo Bay (Spearman rank correlation, $r_s = -0.83$, $P = 0.015$), two different models were run at this location: one with depth removed and one with distance to cable location removed.

Secondly, we used LME regression models with model averaging to determine which temporal environmental variables predict how far fish were from the cable location when first detected at each array. Distance between the receiver that first detected a fish and the cable location was included as the response variable in each LME model per array, while the main fixed effects included cable status (off/on), discharge (log-transformed), tidal current (categorical descriptor), temperature, and a time of day descriptor (binary, day/night) (Table 1). Fish ID was included as a random effect (intercept) in the Benicia and Richmond Bridge models but not in the San Pablo Bay models since no repeated transits per fish ID were observed at this non-bridge location. Due to small sample size at San Pablo Bay for inbound transits, model selection procedures were initially run on two smaller sub-models with the following fixed effects: (1) cable status, discharge, and temperature and (2) cable status, tidal current, and day/night. Variables that were present in the averaged model of each sub-model were then entered together into a final full model for the selection procedure at San Pablo Bay.

Statistical analysis was performed in R 3.6.1 (R Core Team 2021) using primarily the following packages: lme4 (Bates et al. 2015), AICcmodavg (Mazerolle 2020), and MuMIn (Barton 2020). Multicollinearity between the main effect variables in regressions was checked using the variance inflation factor (VIF), and correlated predictors resulting in $VIF > 3$ were removed. Other model assumptions were visually assessed using appropriate plots. Analyses used two-sided tests with 0.05 levels of significance. While all predictor variables present in the final averaged models have some level of influence on the response variable, we defined predictor variables as having a significant level of influence if the 95% confidence intervals of their averaged standardized coefficients did not cross 0 in the LME regression models or if the 95% confidence intervals of their odds ratio did not cross 1 in the logistic regression models.

Results

Study population

The total study sample in the final dataset consisted of 141 adult fish with unique IDs, including 15 females (10.6%), 35 males (24.8%), and 91 of unknown sex (64.5%). Total transits during periods when the cable status was known include 78 inbound transits and 136 outbound transits. These included 73 inbound and 128 outbound unique fish IDs (i.e., not including multiple transits per fish per direction, which occasionally occurred over the years), with 31 fish detected during both inbound and outbound transits. The flowcharts in Fig. 2 enumerate these populations, breaking them down by successful or aborted transits, cable energization status,

and misdirection to the Bay Bridge. Fish detections utilized in this study occurred between October 26, 2006, and February 13, 2015.

Transit success and misdirection

Inbound

Transit success

Of the 73 unique inbound fish, 66 (90.4%) transited successfully through the lower migration route (68 of 78 total transits, 87.2%). From the values in Fig. 2a, the odds of a successful transit post-cable energization (50 success/28 abort) was 7.8 times the odds pre-energization (16/5) [Fisher's exact test, odds ratio (OR) 7.8, 95% confidence interval (CI) 1.4–44, $P < 0.02$], which superficially suggests that the cable positively influenced inbound migration. However, in the expanded model with additional environmental variables considered (Table 2, Table ESM 2), cable status was present in the final model but did not meet the criteria for significance (Logistic regression, $N = 73$, OR 4.73, CI 0.5–42, $P > 0.1$), though remained suggestive. Cable status, discharge, detection at Bay Bridge, and temperature were all present in the final averaged model (Table 2; Table ESM 2), but only water temperature was significantly related to transit success: Fish were more likely to successfully pass inbound through the lower migration route in colder water (logistic regression, $N = 73$, OR 0.08, CI 0.01–0.77, $P < 0.03$).

Misdirection

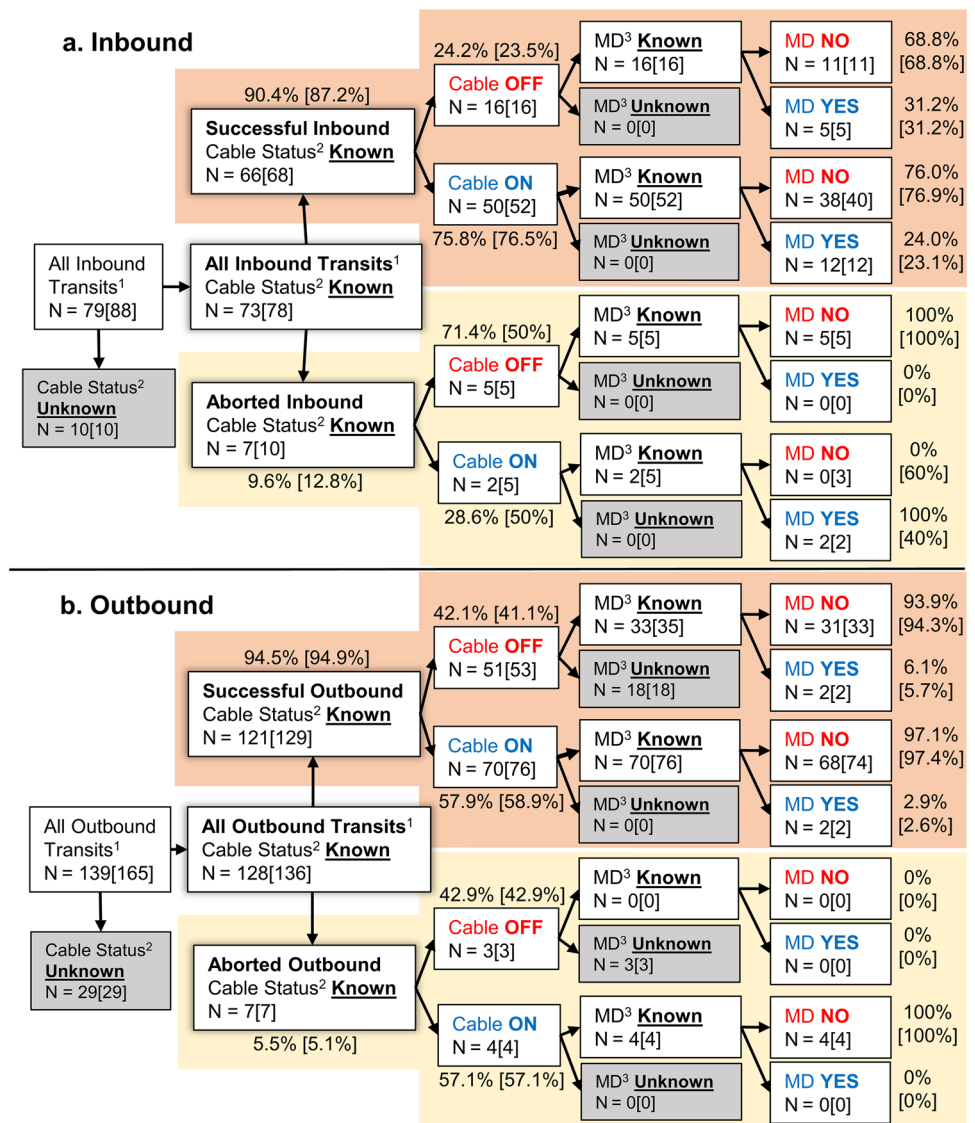
Misdirection to the Bay Bridge was not associated with cable status (off/on) (Fisher's exact test, OR 1.18, CI 0.36–3.8, $P > 0.5$, Fig. 2a). Across the entire study period when the array at the Bay Bridge was active (i.e., after February 10, 2007), there was no association of successful transit with misdirect (success/abort) (Fisher's exact test, OR 0.87, CI 0.15–4.9, $P > 0.5$, Fig. 2a). Of 73 inbound fish, 19 (26.0%) were detected at the Bay Bridge (19 of 78 total transits, 24.4%), and only two of these did not complete a successful transit. No environmental variables significantly predicted the probability of an inbound fish being detected at Bay Bridge, with only discharge present in the averaged model but at a nonsignificant level (Table 2, Table ESM 2).

Outbound

Transit success

Of the 128 outbound fish, 121 (94.5%) transited successfully (129 of 136 total transits, 94.9%). The success of outbound

Fig. 2 Flowchart of detection data for inbound (a) and outbound (b) green sturgeon in relation to cable status, transit success, and misdirection to Bay Bridge. Sample sizes (N) represent the number of unique non-repeated fish in each category, while numbers in brackets show total transits (regardless of repeated observations per fish)



¹Includes both successful and aborted transits. ²Cable status: Detections between January 1 and November 23, 2010, occurred during the operational testing period for the TBC, and therefore, cable energization status was defined as “Unknown” during this time frame. ³MD (Misdirection): Detections before February 10, 2007, occurred when Bay Bridge arrays were not operational, and therefore, misdirect information was defined as “Unknown”

transits was not associated with the cable’s status (Fisher’s exact test, OR 1.03, CI 0.22–4.8, $P > 0.5$, Fig. 2b). In the expanded logistic regression model with additional environmental variables considered (Table 2, Table ESM 2), the final averaged model retained cable status and log (discharge) but at nonsignificant levels.

Misdirection

Outbound misdirection to the Bay Bridge was not associated with either cable status (Fisher’s exact test, OR

0.43; CI 0.06–3.2, $P > 0.5$, Fig. 2b) or successful transit across the entire study period (Fisher’s exact test, OR ∞ , CI 0– ∞ , $P > 0.5$). Of 107 total successful outbound transits occurring when the Bay Bridge array was active, just four (3.7%) were misdirected to the Bay Bridge. In the expanded model, no variables were found to significantly influence the probability of an outbound fish’s detection at the Bay Bridge, although cable status, temperature, and log (discharge) were all present in the averaged model (Table 2, Table ESM 2).

Table 2 Model-averaged results for predictors of successful transit and misdirection for inbound and outbound transits

Response	Predictors ^a	<i>N</i>	Coef	SE	<i>P</i> value	OR	CI	<i>I</i>
Inbound transit								
Successful transit	Intercept	73	3.16	0.73	<0.0001	23.54	5.45–101.63	
	Cable status (on)		1.56	1.09	0.161	4.73	0.54–41.66	0.46
	Temperature		–2.54	1.15	0.029	0.08	0.01–0.77	0.87
	Log (discharge)		2.22	1.86	0.238	9.18	0.23–364.58	0.42
	Misdirect (yes)		–0.57	1.00	0.574	0.56	0.08–4.15	0.11
Misdirect	Intercept	73	–1.05	0.27	0.00012	0.35	0.21–0.60	
	Log (discharge)		–0.33	0.55	0.562	0.72	0.24–2.18	0.29
Outbound transit								
Successful transit	Intercept	109	6.75	731.05	0.993	849.06	0.0–∞	
	Cable status (on)		–17.82	2983.00	0.995	1.82e–8	0.0–∞	0.66
	Log (discharge)		1.96	1.35	0.150	7.09	0.49–102.37	0.57
Misdirect	Intercept	109	–3.30	0.53	<0.0001			
	Cable status (on)		–0.87	1.02	0.400	0.42	0.06–3.18	0.22
	Temperature		–0.40	1.06	0.709	0.67	0.08–5.45	0.16
	Log (discharge)		0.76	1.07	0.482	2.14	0.26–17.75	0.20

Parameter coefficients (Coef), standard errors (SE), *P* values, odds ratios (OR), 95% confidence intervals (CI) of the odds ratio, and relative importance (*I*) were calculated using the natural averaging method on all candidate logistic regression models with $\Delta\text{AICc} < 2$ from the best fit model. Sample sizes (*N*) are provided for each averaged model. Significant predictors (based on CI not crossing 1) are in bold

^aPredictor variables were standardized before model averaging. Reference level for categorical variables include “off” for cable status and “no” for misdirect

Transit time

Transit times through each reach for inbound and outbound GS when the cable was energized and not energized are summarized in Fig. 3, Table ESM 3. Transit times for inbound and outbound fish that were detected or not detected at the Bay Bridge (while the array was active) during transits through the outer and total reaches are summarized in Fig. 4, Table ESM 4. The extreme outliers removed to form the trimmed datasets were only longer transits, representing 1.37–4.29% (1–3 transits removed) of all transits for inbound fish and 0.96–1.923% (1–2 transits removed) of all transits for outbound fish, depending on reach.

Inbound

Transit times of inbound fish through the three reaches during period of cable non-energization vs. energization were not significantly different from each other (Wilcoxon rank sum test; see Fig. 3, Table 3). However, inbound fish that were detected at Bay Bridge took significantly longer to transit through the outer reach (medians of non-detection vs. detection at Bay Bridge: 12.61 h vs. 36.42 h, Wilcoxon rank sum test, $W = 260$, $N = 68$, $P = 0.004$, effect size = 0.34, Fig. 4, Table 3) and the total reach (medians of non-detection vs. detection at Bay Bridge: 47.31 h vs. 75.54 h, Wilcoxon rank sum test, $W = 204$, $N = 65$, $P = 0.001$, effect size = 0.40, Fig. 4, Table 3).

These results were supported in the expanded environmental models of outer and total reach transit times: Fish transited over a greater duration through these reaches if they were detected at Bay Bridge (LME, outer reach: $N = 73$, $\beta = 0.86$, CI 0.43–1.30, $P < 0.0001$, total reach: $N = 70$, $\beta = 0.68$, CI 0.31–1.04, $P = 0.0003$, Table 4, Table ESM 5). No other variables were significantly related to transit time through the outer and total reaches, although nonsignificant variables included cable status and temperature (Table 4, Table ESM 5).

In the inner reach, the lone top model included only temperature as a fixed effect (i.e., there were no other models with $< 2 \Delta\text{AICc}$ from the best fit model, so model averaging was not conducted for this reach). Inbound fish transited through the inner reach in less time when temperatures were lower (LME, $N = 68$, $\beta = 0.38$, CI 0.05–0.71, $P = 0.0245$, Table 4, Table ESM 5).

For the trimmed dataset that excluded extreme outliers in logged transit time, misdirection to Bay Bridge continued to be a significant predictor of longer transit times in the outer and total reaches and temperature still showed a positive significant relationship with transit time through the inner reach (Table ESM 6). Furthermore, temperature became a significant predictor of transit time in the outer reach: Fish transited faster when temperatures were lower (LME, $N = 72$, $\beta = 0.32$, CI 0.0001–0.64, $P = 0.0499$, Table ESM 6). Other model selection results with the trimmed dataset produced minor changes to nonsignificant variables in the reaches:

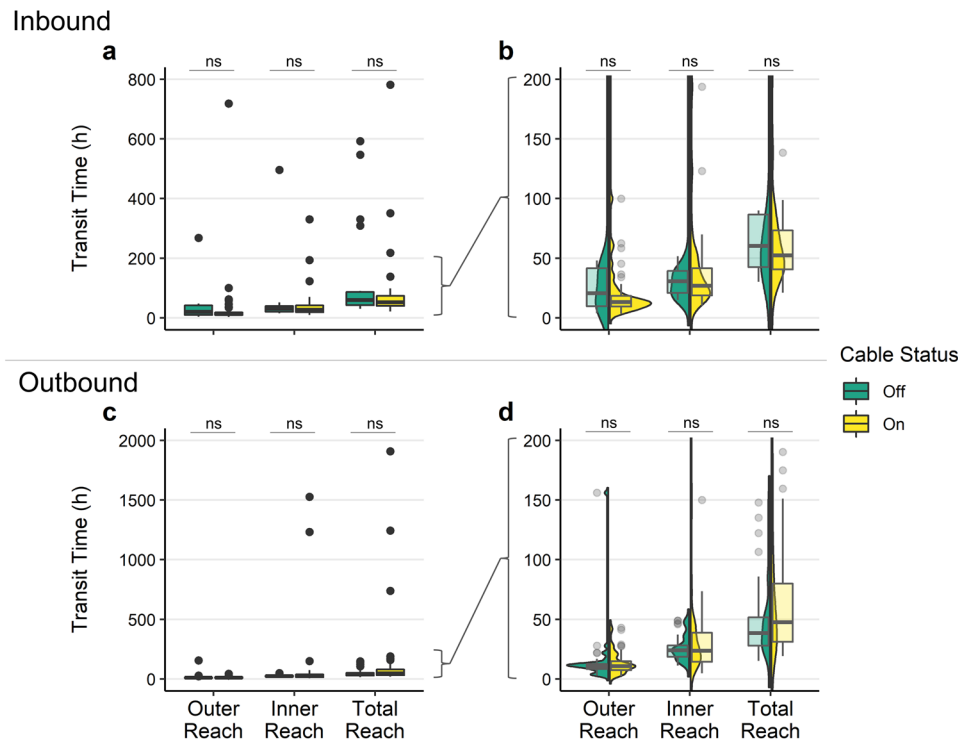


Fig. 3 Transit times of inbound and outbound green sturgeon during periods of cable non-energization and energization. Box plots of transit times (h) from the unique fish non-trimmed datasets during different periods of cable energization status (cable status, off/on) are presented for the outer, inner, and total reaches. The upper row of plots displays the inbound transits (**a**: full data range, **b**: zoomed-in subset showing transit times < 200 h), and the lower row displays the outbound transits (**c**: full data range, **d**: zoomed-in subset showing

transit times < 200 h). Within the zoom plots (**b**, **d**), split violin plots characterize the data distribution within groups using kernel density estimates (curve width indicates the proportion of data points in that region). The first and third quartiles of the box plots are depicted by the lower and upper hinges, the median is the dark midline, and the whiskers extend to values within 1.5 times the interquartile range. Results of Wilcoxon rank sum tests are indicated above each paired comparison: ns = $P > 0.05$, * $P \leq 0.05$, ** $P \leq 0.01$, *** $P \leq 0.001$

Cable status was included as a nonsignificant variable in the inner and outer reaches, temperature in the total reach, and discharge in the outer and total reaches (Table ESM 6).

Outbound

Transit times of outbound fish through the three reaches were not significantly different between periods when the cable was not energized vs. energized (Wilcoxon rank sum test; see Fig. 3, Table 3) or when fish were detected versus not detected at Bay Bridge, regardless of cable status (Wilcoxon rank sum test; see Fig. 4, Table 3). However, in the expanded environmental models, outbound transit times through the total reach were significantly greater with the cable energized (LME, $N = 105$, $\beta = 0.34$, CI 0.01–0.67, $P = 0.046$, Table 4, Table ESM 5). A similar significant relationship was observed in the trimmed dataset that removed two extreme outliers (LME, $N = 102$, $\beta = 0.27$, CI 0.004–0.53, $P = 0.047$, Table ESM 6).

No other environmental variables were significant in any reach within the final averaged models of the full

non-trimmed datasets. Nonsignificant factors included cable status in the inner and outer reaches, temperature and discharge in all reaches, and misdirection to the Bay Bridge in the outer reach (Table 4, Table ESM 5). When the trimmed datasets were utilized, fewer nonsignificant factors were present in the final averaged models: temperature in the inner and outer reaches, discharge in the inner and total reaches, and misdirect in the outer reach (Table ESM 6).

Location of first detection at arrays

Inbound

For inbound fish at the Benicia Bridge, the odds of being detected at a receiver were 97.59% lower for every 1 km increase in the distance from cable location (CLR, $N_{\text{events}} = 66$, OR 0.02, CI 0.004–0.13, $P < 0.0001$, Fig. 5, Table ESM 7), 8.66% higher for every 1 m increase in channel depth (CLR, $N_{\text{events}} = 66$, OR 1.09, CI 1.03–1.15, $P = 0.003$, Fig. 5, Table ESM 7), and 6.32% lower for

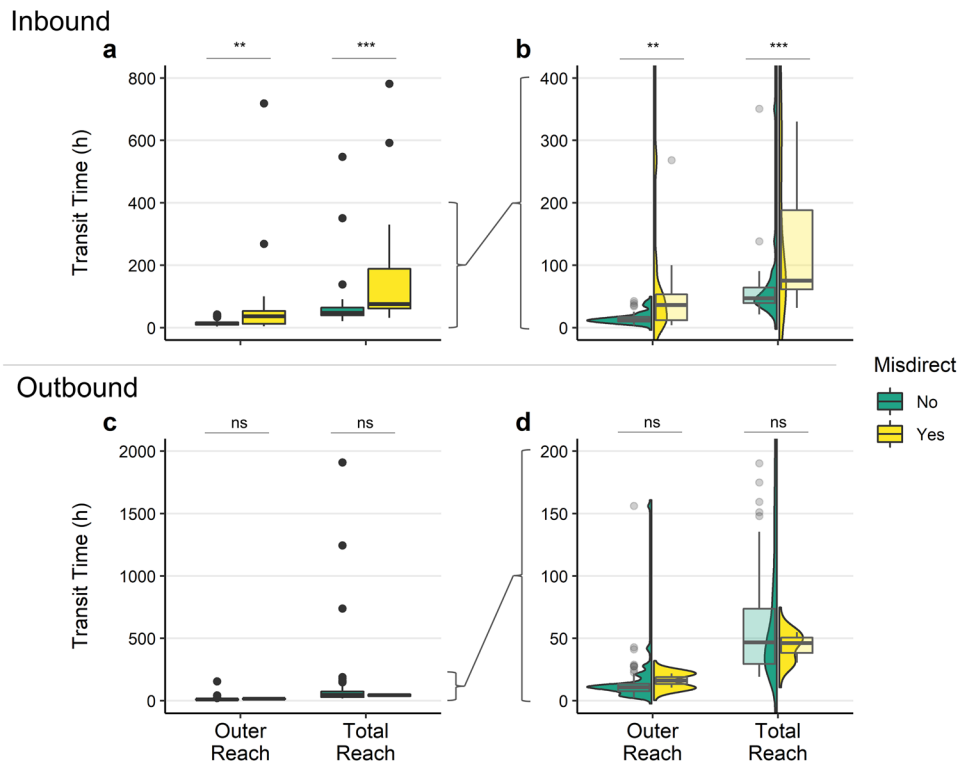


Fig. 4 Transit times of inbound and outbound green sturgeon during transits involving no misdirection or misdirection to Bay Bridge. Box plots of transit times (h) from the unique fish non-trimmed datasets during transits without misdirection or with misdirection (misdirect, no/yes) are presented for the outer and the total reaches. The upper row of plots displays the inbound transits (**a**: full data range, **b**: zoomed-in subset showing transit times <400 h), and the lower row displays the outbound transits (**c**: full data range, **d**: zoomed-in subset showing transit times <200 h). Within the zoom plots (**b**, **d**), split violin plots

characterize the data distribution within groups using kernel density estimates (curve width indicates the proportion of data points in that region). The first and third quartiles of the box plots are depicted by the lower and upper hinges, the median is the dark midline, and the whiskers extend to values within 1.5 times the interquartile range. Results of Wilcoxon rank sum tests are indicated above each paired comparison: ns = $P > 0.05$, * $P \leq 0.05$, ** $P \leq 0.01$, *** $P \leq 0.001$

every 1 unit increase in square root of deep net MF (CLR, $N_{\text{events}} = 66$, OR 0.94, CI 0.90–0.98, $P = 0.004$, Fig. 5, Table ESM 7). At the Richmond Bridge array, inbound fish were also more likely to be first detected in areas with deeper water (CLR, $N_{\text{events}} = 73$, OR 1.17, CI 1.11–1.24, $P < 0.0001$, Fig. 5, Table ESM 7), meaning the odds of detection at a receiver increase by 17.08% for every 1 m increase in channel depth. However, no environmental variables tested were significantly related to where inbound fish were first detected at the non-bridge San Pablo Bay array. Cable status was not significantly associated with distance to cable location at first detection for inbound fish in the conditional logistic regression models.

With respect to temporal environmental variables, the distance to cable location was significantly related to discharge at both bridge locations (LME, Benicia Bridge: $N = 66$, $\beta = 0.06$, CI 0.003–0.12, $P = 0.039$, Richmond Bridge: $N = 73$, $\beta = 0.44$, CI 0.06–0.82, $P = 0.022$, Tables ESM 8, ESM 9): Fish were further from the cable location during periods of higher river discharge. However, discharge was

not present in the final averaged model at the San Pablo array. Cable status (off/on) was included in the final averaged model for inbound fish at each array, indicating that it does have some predictive power relating to how far fish migration paths were from the cable location, but it did not achieve statistical significance (Table ESM 8). Other nonsignificant environmental variables in the final averaged models included temperature (Richmond Bridge and San Pablo Bay), tidal current (San Pablo Bay), and time of day (Benicia Bridge and San Pablo Bay).

Outbound

At the Benicia Bridge array, fish were more likely to be found closer to the cable location (CLR, $N_{\text{events}} = 116$, OR 0.04, CI 0.01–0.20, $P < 0.0001$; detection odds 95.90% lower per 1 km increase in distance to cable) and in areas with lower surface net MF (CLR, $N_{\text{events}} = 116$, OR 0.96, CI 0.92–0.99, $P = 0.012$; detection odds 4.37% lower per 1 unit increase in square root surface total MF) (Fig. 5, Table ESM

Table 3 Wilcoxon rank sum tests of transit time, cable status, and misdirection

Variable	Reach	<i>N</i>	<i>W</i>	DiffLoc	CI	<i>P</i> value	Effect size ^a
Inbound transits							
Cable status	Outer	68 (off = 16, on = 52)	513	5.41	− 2.18 to 22.17	0.163	0.17 [0.01–0.42]
	Inner	63 (16, 47)	393	0.64	− 7.27 to 9.79	0.797	0.03 [0.004–0.28]
	Total	65 (18, 47)	489	7.03	− 7.36 to 25.43	0.340	0.12 [0.01–0.37]
Misdirect	Outer	68 (no = 49, yes = 19)	260	− 19.14	− 32.34 to − 3.61	0.004	0.34 [0.07–0.58]
	Total	65 (47, 18)	204	− 28.20	− 45.58 to − 12.76	0.001	0.40 [0.16–0.59]
Outbound transits							
Cable status	Outer	105 (off = 37, on = 68)	1230	− 0.09	− 2.50 to 1.47	0.854	0.02 [0.003–0.22]
	Inner	106 (36, 70)	1268	0.15	− 5.21 to 3.46	0.960	0.005 [0.003–0.20]
	Total	113 (46, 67)	1271	− 7.18	− 17.77 to 1.39	0.115	0.15 [0.01–0.32]
Misdirect	Outer	97 (no = 95, yes = 2)	63	− 4.53	− 16.03 to 10.10	0.424	0.08 [NA ^b]
	Total	98 (95, 3)	153	1.48	− 20.94 to 53.42	0.837	0.02 [NA ^b]

Tests determined if transit time differed between periods of cable energization (off/on) and different states of misdirection (no/yes). Results include sample size (overall *N*, and *N* for each binary state), *W* statistic (*W*), difference in location of estimates (DiffLoc) with 95% confidence intervals (CI), *P* value, and effect size with 95% confidence intervals in brackets. Significant differences in transit times between groups, indicating that the true location shift of the two distributions is not equal to 0, are in bold

^aEffect size was calculated as the *z* statistic divided by the square root of the sample size. Confidence intervals were generated by bootstrap resampling using 10,000 repetitions

^bBootstrapped confidence intervals not obtained due to low sample size of misdirect “yes” group

7). There was a weak significant interaction between depth and discharge (CLR, $N_{\text{events}} = 116$, OR 0.99, CI 0.99–1.00, $P = 0.013$, Fig. 5, Table ESM 7): Fish were more likely to be first detected in shallower water when river discharge was high. At the Richmond Bridge array, outbound fish were more likely to be first detected closer to the cable location (CLR, $N_{\text{events}} = 117$, OR 0.39, CI 0.31–0.50, $P < 0.0001$, Fig. 5, Table ESM 7; detection odds 60.71% lower per 1 km increase in distance to cable) and in areas with deeper water (CLR, $N_{\text{events}} = 117$, OR 1.14, CI 1.09–1.18, $P < 0.0001$, Fig. 5, Table ESM 7; detection odds 13.60% higher per 1 m increase in channel depth). Similarly, outbound fish at the non-bridge San Pablo Bay array were also more likely to be first detected closer to the cable location (CLR, $N_{\text{events}} = 46$, OR 0.15, CI 0.05–0.46, $P = 0.001$, Fig. 5, Table ESM 7; detection odds 85.14% lower per 1 km increase in distance to cable) and in areas with deeper water (CLR, $N_{\text{events}} = 46$, OR 1.49, CI 1.18–1.87, $P < 0.0001$, Fig. 5, Table ESM 7; detection odds 48.87% higher per 1 m increase in channel depth). Similar to inbound fish, cable status was not significantly associated with distance to cable location at first detection for outbound fish in the conditional logistic regression models.

In our second temporal-based analysis focusing on the distance between cable location and the outbound migration path (i.e., first detection location), none of the environmental variables tested were significantly related to distance from cable at any of the arrays examined (Tables ESM 8, ESM 9). Although cable status was present in the final averaged model at Benicia Bridge and San Pablo Bay (Table ESM 8),

it did not achieve statistical significance. Other nonsignificant environmental variables in the final averaged models included discharge (at all arrays), temperature (bridge arrays only), and time of day (bridge arrays only).

Discussion

The availability of detection data collected along the GS migration route both when the TBC was energized and not energized permitted an assessment of whether the energized cable—and by inference the MF from its load—may have affected GS migratory behavior.

Effect of cable

Overall, the evidence of any effects due to cable status (off/on) was varied. When only considering cable status, inbound fish were more likely to successfully transit through the study region when the cable was energized than when it was not (96.2% vs. 76.2%, for unique fish IDs), while the odds of successful outbound transits were not significantly related to cable status. Inbound and outbound transit times were not significantly different when the cable was energized vs. not energized in any of the three reaches (inner, outer, total) when using the unique ID dataset and only considering the effect of cable energization. However, in the expanded environmental model which included repeated transits per fish, fish took more time to transit out through the total reach when the cable was energized. The migration path of

Table 4 Model-averaged results for predictors of transit time

Response	Predictors ^a	<i>N</i>	Coef	SE	CI	<i>P</i> value	<i>I</i>
Inbound transit							
Outer reach time	Intercept	73	2.78	0.10	2.59 to 2.98	<0.0001	
	Cable status (on)		-0.20	0.20	-0.59 to 0.19	0.313	0.26
	Temperature		0.22	0.17	-0.12 to 0.57	0.207	0.26
	Misdirect (yes)		0.86	0.22	0.43 to 1.30	<0.0001	1.0
Inner reach time ^b	Intercept	68	3.44	0.09	3.27 to 3.61	<0.0001	
	Temperature		0.38	0.17	0.05 to 0.71	0.0245	NA
Total reach time	Intercept	70	4.15	0.08	3.99 to 4.31	<0.0001	
	Cable status (on)		-0.30	0.17	-0.64 to 0.04	0.084	0.56
	Temperature		0.28	0.16	-0.03 to 0.60	0.074	0.59
	Misdirect (yes)		0.68	0.18	0.31 to 1.04	0.0003	1.00
Outbound transit							
Outer reach time	Intercept	104	2.36	0.06	2.23 to 2.49	<0.0001	
	Cable status (on)		-0.11	0.14	-0.39 to 0.16	0.423	0.19
	Temperature		0.13	0.13	-0.13 to 0.38	0.331	0.16
	Log (discharge)		-0.06	0.13	-0.32 to 0.19	0.627	0.13
	Misdirect (yes)		0.37	0.47	-0.56 to 1.29	0.439	0.16
Inner reach time	Intercept	104	3.25	0.08	3.09 to 3.39	<0.0001	
	Cable status (on)		0.13	0.14	-0.15 to 0.41	0.350	0.21
	Temperature		0.16	0.15	-0.13 to 0.45	0.288	0.24
	Log (discharge)		0.09	0.14	-0.19 to 0.36	0.548	0.16
Total reach time	Intercept	105	3.95	0.08	3.80 to 4.10	<0.0001	
	Cable status (on)		0.34	0.17	0.01 to 0.67	0.046	0.78
	Temperature		0.28	0.16	-0.04 to 0.60	0.089	0.63
	Log (discharge)		-0.17	0.17	-0.50 to 0.15	0.299	0.29

Parameter coefficients (Coef), standard errors (SE), 95% confidence interval (CI) of the coefficient, *P* values, and relative importance (*I*) were calculated using the natural averaging method on all candidate linear mixed-effects regression models with $\Delta AICc < 2$ from the best fit model. Sample sizes (*N*) are provided for each averaged model. Significant predictors (based on CI not crossing 0) are in bold

^aPredictor variables were standardized before model averaging. Reference level for categorical variables include “off” for cable status and “no” for misdirect

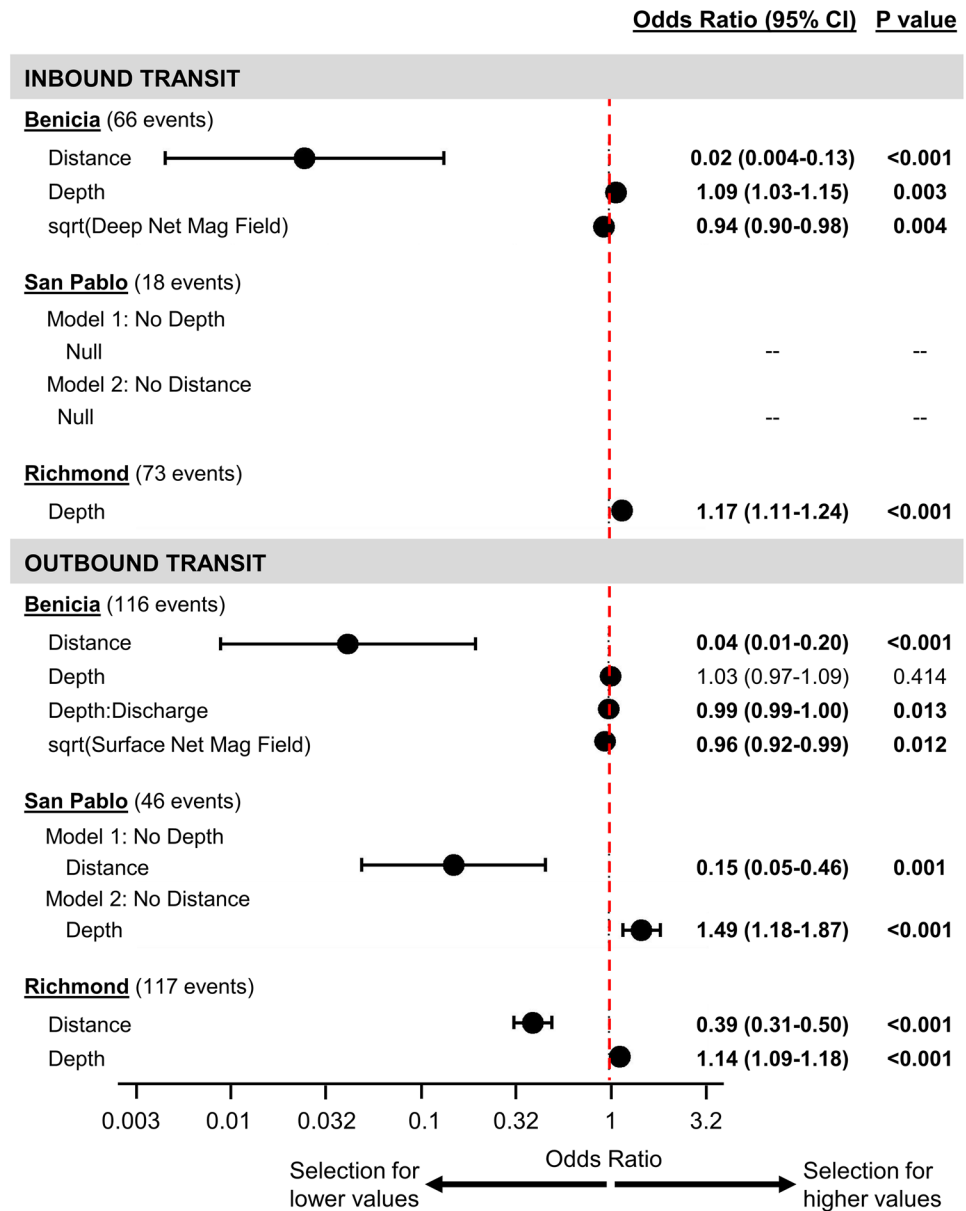
^bResults represent the best fitting model only as no other model was < 2 $\Delta AICc$ values from the best fit model

inbound and outbound GS was not significantly related to the cable’s energization status at the three locations examined (Benicia Bridge, Richmond Bridge, San Pablo Bay). In other words, when fish first approached each array, their distance to the cable location was not strongly influenced by the cable’s energization status. However, it is worth noting that cable status was retained as a nonsignificant predictor in most of the expanded models (i.e., models including other environmental variables) of transit success, transit time, and migration path location for both transit directions. These results suggest that cable status has some predictive power on these measures of migration behavior, but that it did not reach the level of significance. While this study investigates the potential influence of a single HVDC cable, more complex configurations of marine resource technology, e.g., inter-array cable connections and export cables of a marine wind farm (Hutchison et al. 2020a), may lead to

repeated or chronic exposure to anthropogenic EMF, resulting in stronger effects on movement and migration behaviors. Thus, additional data across a range of marine energy configurations are required to more fully investigate any potential effects of anthropogenic EMF.

It is unknown why the energized cable was associated with increased transit success for inbound GS while having no association for outbound GS transit success. The possibility that the energized cable, which runs mostly parallel to the migration route in this region, enabled more successful inbound transits by serving as a potential navigational aid (e.g., via topotaxis) or source of attraction may be unlikely since inbound fish were not detected closer to the cable or transiting in shorter durations when the cable was energized. However, further study on the navigational cues used by migrating GS, as well as potential attraction or avoidance of anthropogenic EMF sources, is strongly advised.

Fig. 5 Forest plot of odds ratios for environmental variables associated with the location of first detection. Estimated odds ratios (exponentiated coefficients) with 95% confidence interval (CI) are provided for the best fit conditional logistic regression model for each array and transit direction combination. Significant parameters ($P < 0.05$) are in bold, and their placement left or right of the dashed line indicates the direction of the selection. CI located left of the dashed line indicates selection for lower values of the environmental variable (i.e., detection is more likely at lower values of that variable), while CI right of the dashed line indicates selection for higher values (i.e., detection is more likely at higher values of that variable)



Regarding outbound transits, Wyman et al. (2018a) used a similar methodology to investigate the TBC’s potential effect on the outmigration behaviors of juvenile Chinook salmon, an MF-sensitive species (Putman et al. 2014a) whose general migration route through the SF Bay is highly similar to adult GS. Similar to outbound GS results, transit success of outbound salmon was not related to cable energization. In a small-scale tracking study of EMF-sensitive European eels, Westerberg and Begout-Anras (2000) found that approximately 60% of eels monitored passed over an HVDC cable similar to the TBC during their migration route, indicating that the cable’s EMF did not act as a strong barrier to their regular migration movements.

Our results of increased outbound transit durations in association with cable energization may be supported by

some field and laboratory-based studies that examined changes in movement and swimming behaviors of EMF-sensitive species in relation to actual or replicated subsea power cables. Field studies of migrating European eels found that eels showed brief alterations to their directional movement as they crossed an HVDC cable (Westerberg and Begout-Anras 2000) and that eels slowed down significantly as they passed over the region of an AC cable as compared to swim speeds further away on either side of the cable (Westerberg and Lagenfelt 2008). In situ enclosure studies demonstrated that little skates (*Leucoraja erinacea*) decreased swim speeds and increased exploratory behaviors in the presence of an energized HVDC cable similar to the TBC (Hutchison et al. 2020b). In semi-natural mesocosm experiments, some elasmobranch species showed reduced movements and

increased presence near an energized AC cable (Gill et al. 2009). In laboratory experiments, Bevelhimer et al. (2013) exposed juvenile paddlefish (*Polyodon spathula*) and lake sturgeon to the rapid onset of a strong, variable EMF created by an AC electromagnet, effectively simulating swimming encounters with hydrokinetic projects such as power transmission cables. While paddlefish showed no reaction, lake sturgeon exhibited altered swimming behavior, including slower swim speeds and pausing or suddenly stopping near the magnet (Bevelhimer et al. 2013). However, other studies demonstrate different behavioral associations or no associations at all to cable energization. For example, a field study of similar design in the same region showed that juvenile Chinook salmon exhibited decreased outbound transit durations after the TBC was energized (Wyman et al. 2018a). And pallid sturgeon (*Scaphirhynchus albus*) showed no significant differences in large-scale movements or attraction/avoidance behaviors in response to AC-generated MFs representative of undersea power cables in mesocosm trials (Bevelhimer et al. 2015). While it is unknown what exact behavioral changes, or the mechanisms behind them, were responsible for our observations of increased outbound transit durations by migrating GS during active cable periods, it is possible that exposure to the cable-generated MF caused altered swim behaviors, decreased swim speeds, or increased periods of holding or exploratory behavior near the cable, ultimately resulting in increased transit durations through SF Bay. However, transit times of inbound GS were not related to cable energization, potentially indicating that the reproductive drive of fish on their way to the upstream spawning grounds was stronger than the possible behavioral influence of cable-based MF.

Additionally, “magnetic displacement” or exposure experiments have demonstrated how alterations to the Earth’s natural geomagnetic fields (such as distortions or perturbations caused by anthropogenic EMF) can affect the navigation and orientation behaviors of species that use geomagnetic cues as a map, compass, or topotaxis guide during migration or local movements (see Nyqvist et al. 2020; Klimley et al. 2021 for review). Juvenile European eels (Naisbett-Jones et al. 2017) and bonnethead sharks (*Sphyrna tiburo*) (Keller et al. 2021) will change their orientational behavior after brief exposures (10–15 min) to relatively minor changes of < 5–10% in magnetic intensity and inclination. Magnetic displacement experiments in juvenile pink salmon (*Oncorhynchus gorbuscha*) that simulated different locations along their migratory route demonstrate that an innate use of a magnetic map drives their large-scale migrations (Putman et al. 2020). Exposure to anthropogenic MFs that create sharp gradients in the rearing or incubation environment subsequently disrupts the ability to correctly respond to magnetic displacements in juvenile steelhead trout (*Oncorhynchus mykiss*) (Putman et al. 2014b) and

hatchling loggerhead turtles (*Caretta caretta*) (Fuxjager et al. 2014). In juvenile Chinook salmon, strong (85 mT) but brief magnetic pulses alter magnetic orientation behaviors (Naisbett-Jones et al. 2020). Even brief or small alterations to natural MFs may have serious effects on individuals or impacts at the population or ecosystem level if exposure causes orientation or navigation errors at a crucial time or location, depending on the life stage of the animal and the population size, distribution, and ecology (e.g., sensory, reproductive, and feeding ecology) of the species (Nyqvist et al. 2020).

It is important to note that since swimming depth data for the fish in our study were not available for any array, the vertical location of these fish in the water column was unknown for these detections. Such information would be particularly useful in assessing fish behavior in relation to potential exposure to MF anomalies generated by the cable and other environmental factors. Channel depth was approximately 13 m where the TBC was located at the Richmond Bridge, San Pablo Bay, and Benicia Bridge arrays. Chapman et al. (2019) observed detections of nine adult GS with depth sensors in SF Bay and suggested they were benthically orientated as 77% of detections were at depths greater than 10 m. Although the migration status of these fish was unknown, these observations suggest that adult GS may naturally swim closer to the channel bottom where the cable’s MF anomaly would be stronger. Furthermore, a manual tracking study of non-migrating GS (five sub-adults, one adult) in SF Bay indicated that fish generally swam with non-directional movements near the channel bottom and directional movements near the surface (Kelly et al. 2007). These behaviors were often related to tidal current direction and speed and appeared to reduce the energetic cost of transport experienced by fish (Kelly et al. 2020). While these results may have limited direct application to adult GS behaviors during directed migration movements, there is evidence that other migrating species may employ swimming tactics in tidal areas that reduce energetic expenditure, i.e., swimming with the tidal current toward spawning grounds and resting near the bottom when the current flows in the opposite direction (plaice, *Pleuronectes plates*, Metcalfe et al. 1990). Such movements could also impact the periodicity and intensity of exposure to cable-generated EMF and therefore are important to assess in this context.

This study focused on the potential influence of cable-generated MF perturbations on GS migratory behavior, but it is also possible that induced EFs associated with subsea cables may have an effect on movement behavior during migration in electrosensitive species like sturgeon (see review Newton et al. 2019; Nyqvist et al. 2020; England and Robert 2022). While long-distance migration movements are more typically associated with magnetoreception (see reviews Walker et al. 2002; Putman 2018; Klimley et al.

2021; Lohmann et al. 2022, but see Newton et al. 2019 and England and Robert 2022), much remains unknown about the exact mechanisms and thresholds of EMF detection and use. As such, the potential influence of induced EFs on GS migration movements cannot be ruled out and future studies should aim to address this issue if possible (see Anderson et al. 2017).

Effect of other factors

A higher percentage of GS was detected at Bay Bridge (i.e., misdirection) during inbound than outbound transits (24.4% vs. 3.4% total transits, respectively) but for both directions, detection at Bay Bridge was not significantly related to transit success and neither cable energization status nor any other tested environmental variable was significantly related to the odds of misdirection. While it is unknown why some fish deviate south to Bay Bridge from their typical migration route, detection at Bay Bridge did significantly increase transit time for inbound (but not outbound) fish through the outer and total reach by factors of 2.4 and 2.0, respectively. It is possible that these “misdirected” fish require additional time to re-orientate themselves toward their natural migration route, especially when they are still relatively close to the mouth of the SF Bay where riverine cues may be weaker.

Water temperature was significantly related to both migration success and transit time for inbound but not outbound GS: Inbound fish were more likely to successfully transit and transit more quickly in colder water. Average temperatures during inbound and outbound transits ranged from 7.3 to 22.1 °C. While optimal thermal ranges and preferences for migrating adult GS have not been sufficiently evaluated, Colborne et al. (2022) determined in a large-scale biotelemetry study that inbound adult GS spawning migrations were initiated as water temperatures start to increase at the end of winter, whereas outbound timing was not related to temperature. While the end of winter may trigger inbound migrations, high temperatures in the incubation and rearing environment can have serious detrimental effects on early life stages (> 16–19 °C, depending on stage), such as reduced hatching success and growth and increased larval deformities and expression of heat shock proteins (reviewed in Rodgers et al. 2019). Thus, our observed pattern of more successful inbound migrations through the SF Bay in colder temperatures may be associated with the drive to reach upstream spawning sites during optimal thermal ranges for early life stages (Colborne et al. 2022). The increased number of unsuccessful (aborted) inbound migrations in warmer temperatures may reflect the ability of sturgeon to abort energetically costly migrations when environmental conditions, e.g., temperature, are not optimal for spawning success and offspring survival. Such selection pressures may be responsible for the importance of temperature over cable

status in the expanded environmental models for inbound fish. Furthermore, our observations of longer inbound transit durations in warmer water may be related to temperature effects on fish bioenergetics. Temperature increases (from 19 to 24 °C) were associated with decreased swimming performance in yearling juvenile green sturgeon (Mayfield and Cech 2004). However, swimming performance in relation to temperature has not been assessed in adults (Rodgers et al. 2019) and temperature was not related to transit duration of outbound fish.

The other environmental variables that were significantly related to migration path locations (i.e., location of first detection at arrays) depended on array location. Overall, similar spatial and temporal variables affected both inbound and outbound migration paths and were more important at the bridge arrays than the non-bridge array. Regarding spatially related variables, migration paths near bridge arrays were more likely to be closer to the cable location regardless of energization status (in: Benicia only, out: both bridges) and where channel depth was high (in: both bridges, out: Richmond only). At Benicia Bridge, the migration path was more likely to be in areas with lower net MF magnitudes (i.e., closer to the geomagnetic field) near the channel bottom (inbound) and near the surface (outbound). Regarding the effect of temporal-based environmental variables on the location of first detection at bridge arrays, fish were more likely to be further from the cable (inbound fish) or in shallower water (outbound fish) during periods of high water discharge from inland regions. At the non-bridge array, no spatial or temporal environmental variables influenced the location of inbound migration paths, but outbound fish were more likely to be first detected at receivers closer to the cable location (regardless of energization status) and where channel depth was high. Again, data on fish depth in the vertical water column would be highly informative for our study results involving other environmental factors that may be associated with movement behavior.

Conclusion

Overall, there was varied evidence for an association between cable status (off/on) and migration behavior of adult green sturgeon through the lower portion of their migration route. The results indicate that a higher percentage of inbound fish were able to successfully transit inbound after the cable was energized, but this effect was nonsignificant in models that included temperature. Outbound fish took longer to transit when the cable was energized. Inbound and outbound migration paths were not significantly influenced by the cable’s energization status, but model results suggest a potential subtle relationship between cable energization and the location of both inbound and outbound fish migration

paths. While our results do not show a strong negative effect on adult green sturgeon migratory behavior and success, we urge further study on the potential effects (and population-level impacts) of anthropogenic EMFs on this threatened population, for instance, on the behavior of juveniles and subadults during their seasonal movements and utilization of the SF Bay (Miller et al. 2020).

Given the observational and experimental evidence supporting the influence of anthropogenic EMF sources on marine species behavior, we strongly recommend that more research should be carried out in future on this topic. This is especially important given the strong trend for increased use of marine environments for energy sourcing and transport. See Gill and Desender (2020), Hutchison et al. (2020a), Nyqvist et al. (2020), and Klimley et al. (2021) for reviews and recommended studies. Future research should include a variety of species, life stages, behavioral categories (e.g., migrations, foraging, reproduction, predator avoidance, etc.), and ecosystems. We agree with Westerberg and Lagenfeldt (2008) that intensive tracking studies are necessary to identify effects on a migratory species. Future tracking studies should employ transmitters carrying a strain gauge, 3-axis accelerometer, 3-axis magnetometer, and depth gauge to characterize the swimming behavior of the fish and field strength as they pass near or over undersea power cables. Such studies are especially important in tidal areas as this may impact fish movement and depth and, thus, the potential timing and intensity of exposure to cable-generated EMF. Furthermore, it would be beneficial to examine behavioral changes associated with induced EFs in addition to MFs generated by subsea cables (Newton et al. 2019; Gill and Desender 2020; Nyqvist et al. 2020). Additionally, it is important to examine species behavior in relation to a range of subsea cable properties and configurations since many previous studies, including this one, have examined species responses to a single cable or EMF source. For example, it would be highly interesting to assess behavioral responses to a more complex EMF landscape, such as those produced by a network of dynamic inter-array and export cables associated with floating marine wind farms, as repeated exposure may culminate in stronger behavioral effects.

Supplementary Information The online version contains supplementary material available at <https://doi.org/10.1007/s00227-023-04302-4>.

Acknowledgements We would like to kindly thank Trans Bay Cable LLC for providing cable load data for this study. We also thank the staff at Geometrics for their training and support (especially Mikhail Tchernychev, Ross Johnson, Randl Rivera, and Naiema Jackson) and the University of California-Davis Biotelemetry Laboratory for their help and support (particularly Michael Thomas and Gabriel Singer). We would also like to thank Ximena Vergara of the Electric Power Research Institute for her help and support with the grant administration. The scope of this project would not be possible without the generous permission to use fish detection data from the National Marine Fisheries Service (Mary Moser), US Bureau of Reclamation (Robert

Chase), California Department of Water Resources (Alicia Seesholtz), Oregon Department of Fish and Wildlife (Erick Van Dyke), Washington Department of Fish and Wildlife (Phillip Dionne, Olaf Langness), and Natural Resource Scientists, Inc. (Dave Vogel). Finally, we thank our editor Dr. Ewan Hunter and two anonymous reviewers for their helpful comments which improved the quality of this manuscript.

Author contributions Study conception and funding acquisition were performed by APK and RK. Study design was performed by APK, MTW, and RK. Data collection and processing were conducted by MTW, RDB, TVA, EDC, PJH, and MDP. Analysis and initial manuscript preparation were performed by MTW. Subsequent manuscript edits were performed by MTW, RK, APK, EDC, PJH, and MDP. All authors approved the final version of the manuscript.

Funding Open access funding provided by University of Zurich. This study was funded by the US Department of Energy, Office of Energy Efficiency and Renewable Energy, award no. DE-EE0006382 and by the US Department of the Interior, Bureau of Ocean Energy Management, Environmental Studies Program, Washington, DC, through Interagency Agreement Number M14PG00012. It was funded through a cost-share agreement with the Electric Power Research Institute (Project 1–105902).

Data availability Fish detection data used in this study are available by request. Environmental data sources are outlined in Table 1.

Declarations

Conflict of interest The authors have no relevant financial or nonfinancial interests to disclose.

Ethics approval All applicable international, national, and/or institutional guidelines for the care and use of animals were followed for data used in association with this study, including University of California Davis Institutional Animal Care and Use Protocols.

Open Access This article is licensed under a Creative Commons Attribution 4.0 International License, which permits use, sharing, adaptation, distribution and reproduction in any medium or format, as long as you give appropriate credit to the original author(s) and the source, provide a link to the Creative Commons licence, and indicate if changes were made. The images or other third party material in this article are included in the article's Creative Commons licence, unless indicated otherwise in a credit line to the material. If material is not included in the article's Creative Commons licence and your intended use is not permitted by statutory regulation or exceeds the permitted use, you will need to obtain permission directly from the copyright holder. To view a copy of this licence, visit <http://creativecommons.org/licenses/by/4.0/>.

References

- Adams PB, Grimes C, Hightower JE, Lindley ST, Moser ML, Parsley MJ (2007) Population status of North American green sturgeon, *Acipenser medirostris*. *Environ Biol Fishes* 79:339–356. <https://doi.org/10.1007/s10641-006-9062-z>
- Anderson JM, Clegg TM, Véras LVMVQ, Holland KN (2017) Insight into shark magnetic field perception from empirical observations. *Sci Rep* 7:11042. <https://doi.org/10.1038/s41598-017-11459-8>
- Barton K (2020) MuMIn: multi-model inference. In: R package version 1.43.17. The comprehensive R archive network (CRAN), Vienna,

- Austria. <https://CRAN.R-project.org/package=MumIn>. Accessed 18 Oct 2021
- Basov BM (1999) Behavior of sterlet *Acipenser ruthenus* and Russian sturgeon *A. gueldenstaedtii* in low-frequency electric fields. *Vopr Ikhtiol* 39:819–824
- Bates D, Mächler M, Bolker B, Walker S (2015) Fitting linear mixed-effects models using lme4. *J Stat Softw* 67:1–48
- Beamesderfer RCP, Simpson ML, Kopp AGJ, Ae RCPB, Simpson ML, Gabriel AE, Kopp J (2007) Use of life history information in a population model for Sacramento green sturgeon. *Environ Biol Fish* 79:315–337. <https://doi.org/10.1007/s10641-006-9145-x>
- Benson RL, Turo S, McCovey BW (2007) Migration and movement patterns of green sturgeon (*Acipenser medirostris*) in the Klamath and Trinity rivers, California, USA. *Environ Biol Fishes* 79:269–279. <https://doi.org/10.1007/S10641-006-9023-6/METRICS>
- Bevelhimer MS, Cada GF, Fortner AM, Schweizer PE, Riemer K (2013) Behavioral responses of representative freshwater fish species to electromagnetic fields. *Trans Am Fish Soc* 142:802–813. <https://doi.org/10.1080/00028487.2013.778901>
- Bevelhimer MS, Cada GF, Scherelis C (2015) Effects of electromagnetic fields on behavior of largemouth bass and pallid sturgeon in an experimental pond setting. ORNL/TM-2015/580. Oak Ridge National Laboratory: Oak Ridge, TN, USA. <https://tethys.pnnl.gov/sites/default/files/publications/Bevelhimer-et-al-2015.pdf>. Accessed 28 May 2023
- Burnham KP, Anderson DR (2002) Model selection and multimodel inference: a practical information-theoretic approach, 2nd edn. Springer, New York
- Chapman ED, Miller EA, Singer GP, Hearn AR, Thomas MJ, Brostoff WN, LaCivita PE, Klimley AP (2019) Spatiotemporal occurrence of green sturgeon at dredging and placement sites in the San Francisco estuary. *Environ Biol Fishes* 102:27–40. <https://doi.org/10.1007/s10641-018-0837-9>
- Colborne SF, Sheppard LW, O'Donnell DR, Reuman DC, Walter JA, Singer GP, Kelly JT, Thomas MJ, Rypel AL (2022) Intraspecific variation in migration timing of green sturgeon in the Sacramento River system. *Ecosphere*. <https://doi.org/10.1002/ecs2.4139>
- Dormann CF, Calabrese JM, Guillaera-Arroita G, Matechou E, Bahn V, Bartoń K, Beale CM, Ciuti S, Elith J, Gerstner K, Guelat J, Keil P, Lahoz-Monfort JJ, Pollock LJ, Reineking B, Roberts DR, Schröder B, Thuiller W, Warton DI, Wintle BA, Wood SN, Wüest RO, Hartig F (2018) Model averaging in ecology: a review of Bayesian, information-theoretic, and tactical approaches for predictive inference. *Ecol Monogr* 88:485–504. <https://doi.org/10.1002/ecm.1309>
- England SJ, Robert D (2022) The ecology of electricity and electroreception. *Biol Rev* 97:383–413. <https://doi.org/10.1111/brv.12804>
- Erickson DL, Webb MAH (2007) Spawning periodicity, spawning migration, and size at maturity of green sturgeon, *Acipenser medirostris*, in the Rogue River, Oregon. *Environ Biol Fishes* 79:255–268. <https://doi.org/10.1007/s10641-006-9072-x>
- Formicki K, Korzelecka-Orkisz A, Tański A (2019) Magnetoreception in fish. *J Fish Biol* 95:73–91. <https://doi.org/10.1111/jfb.13998>
- Fortin D, Fortin M-E, Beyer HL, Duchesne T, Courant S, Dancose K (2009) Group-size-mediated habitat selection and group fusion-fission dynamics of bison under predation risk. *Ecology* 90:2480–2490. <https://doi.org/10.1890/08-0345.1>
- Fuxjager MJ, Davidoff KR, Mangiamele LA, Lohmann KJ (2014) The geomagnetic environment in which sea turtle eggs incubate affects subsequent magnetic navigation behaviour of hatchlings. *Proc R Soc B Biol Sci* 281:20141218. <https://doi.org/10.1098/rspb.2014.1218>
- Gelman A (2008) Scaling regression inputs by dividing by two standard deviations. *Stat Med* 27:2865–2873. <https://doi.org/10.1002/sim.3107>
- Gibbs MA, Northcutt RG (2004) Development of the lateral line system in the shovelnose sturgeon. *Brain Behav Evol* 64:70–84. <https://doi.org/10.1159/000079117>
- Gill AB, Desender M (2020) Risk to animals from electromagnetic fields emitted by electric cables and marine renewable energy devices. In: Copping AE, Hemery LG (eds) OES-environmental 2020 state of the science report: environmental effects of marine renewable energy development around the world. Report for Ocean Energy Systems (OES). Tethys Pacific Northwest National Laboratory, pp 86–103. <https://tethys.pnnl.gov>, <https://doi.org/10.2172/1633088>
- Gill AB, Huang Y, Gloyne-Philips I, Metcalfe J, Quayle V, Spencer J, Wearmouth V (2009) COWRIE 2.0 Electromagnetic fields (EMF) Phase 2: EMF-sensitive fish response to EM emissions from sub-sea electricity cables of the type used by the offshore renewable energy industry. Commissioned by COWRIE Ltd (project reference COWRIE-EMF-1-06)
- Gill AB, Bartlett M, Thomsen F (2012) Potential interactions between diadromous fishes of UK conservation importance and the electromagnetic fields and subsea noise from marine renewable energy developments. *J Fish Biol* 81:664–695. <https://doi.org/10.1111/j.1095-8649.2012.03374.x>
- Gill AB, Gloyne-Philips I, Kimber J, Sigray P (2014) Marine renewable energy, electromagnetic (EM) fields and EM-sensitive animals. In: Shields M, Payne A (eds) Marine renewable energy technology and environmental interactions, humanity and the sea. Springer, Dordrecht, pp 61–79
- Grueber CE, Nakagawa S, Laws RJ, Jamieson IG (2011) Multimodel inference in ecology and evolution: challenges and solutions. *J Evol Biol* 24:699–711. <https://doi.org/10.1111/j.1420-9101.2010.02210.x>
- Heublein JC, Kelly JT, Crocker CE, Klimley AP, Lindley ST (2009) Migration of green sturgeon, *Acipenser medirostris*, in the Sacramento River. *Environ Biol Fishes* 84:245–258. <https://doi.org/10.1007/s10641-008-9432-9>
- Hutchison ZL, Secor DH, Gill AB (2020a) The interaction between resource species and electromagnetic fields associated with electricity production by offshore wind farms. *Oceanography* 33:96–107. <https://doi.org/10.5670/oceanog.2020.409>
- Hutchison ZL, Gill AB, Sigray P, He H, King JW (2020b) Anthropogenic electromagnetic fields (EMF) influence the behaviour of bottom-dwelling marine species. *Sci Rep* 10:4219. <https://doi.org/10.1038/s41598-020-60793-x>
- Hutchison ZL, Gill AB, Sigray P, He H, King JW (2021) A modelling evaluation of electromagnetic fields emitted by buried sub-sea power cables and encountered by marine animals: considerations for marine renewable energy development. *Renew Energy* 177:72–81. <https://doi.org/10.1016/j.renene.2021.05.041>
- Kavet R, Wyman MT, Klimley AP (2016) Modeling magnetic fields from a DC power cable buried beneath San Francisco Bay based on empirical measurements. *PLoS One* 11:1–21. <https://doi.org/10.1371/journal.pone.0148543>
- Keller BA, Putman NF, Grubbs RD, Portnoy DS, Murphy TP (2021) Map-like use of Earth's magnetic field in sharks. *Curr Biol* 31:2881–2886.e3. <https://doi.org/10.1016/j.cub.2021.03.103>
- Kelly JT, Klimley AP, Crocker CE (2007) Movements of green sturgeon, *Acipenser medirostris*, in the San Francisco Bay estuary, California. *Environ Biol Fishes* 79:281–295. <https://doi.org/10.1007/s10641-006-0036-y>
- Kelly JT, Lankford SE, Cech JJ, Klimley AP (2020) Estimating the energetic savings for green sturgeon moving by selective tidal stream transport. *Environ Biol Fishes* 103:455–463. <https://doi.org/10.1007/s10641-020-00969-6>
- Kimber JA, Sims DW, Bellamy PH, Gill AB (2011) The ability of a benthic elasmobranch to discriminate between biological and

- artificial electric fields. *Mar Biol* 158:1–8. <https://doi.org/10.1007/s00227-010-1537-y>
- Klimley AP (1993) Highly directional swimming by scalloped hammerhead sharks, *Sphyrna lewini*, and subsurface irradiance, temperature, bathymetry, and geomagnetic field. *Mar Biol* 117:1–22. <https://doi.org/10.1007/BF00346421>
- Klimley AP, Wyman MT, Kavet R (2017) Chinook salmon and green sturgeon migrate through San Francisco Estuary despite large distortions in the local magnetic field produced by bridges. *PLoS One*. <https://doi.org/10.1371/journal.pone.0169031>
- Klimley AP, Putman NF, Keller BA, Noakes D (2021) A call to assess the impacts of electromagnetic fields from subsea cables on the movement ecology of marine migrants. *Conserv Sci Pract*. <https://doi.org/10.1111/csp2.436>
- Lindley ST, Moser ML, Erickson DL, Belchik M, Welch DW, Rechisky EL, Kelly JT, Heublein J, Klimley AP (2008) Marine migration of North American green sturgeon. *Trans Am Fish Soc* 137:182–194. <https://doi.org/10.1577/t07-055.1>
- Lohmann KJ, Goforth KM, Mackiewicz AG, Lim DS, Lohmann CMF (2022) Magnetic maps in animal navigation. *J Comp Physiol A Neuroethol Sens Neural Behav Physiol* 208:41–67
- Mayfield RB, Cech JJ (2004) Temperature effects on green sturgeon bioenergetics. *Trans Am Fish Soc* 133:961–970. <https://doi.org/10.1577/t02-144.1>
- Mazerolle MJ (2020) AICcmodavg: model selection and multimodel inference based on (Q)AIC(c). R package version 2.3-1. The comprehensive R archive network (CRAN), Vienna, Austria. <https://cran.r-project.org/package=AICcmodavg>. Accessed 14 May 2021
- Metcalf JD, Arnold GP, Webb PW (1990) The energetics of migration by selective tidal stream transport: an analysis for plaice tracked in the southern north sea. *J Mar Biol Assoc UK* 70:149–162. <https://doi.org/10.1017/S0025315400034275>
- Meyer CG, Holland KN, Papastamatiou YP (2005) Sharks can detect changes in the geomagnetic field. *J R Soc Interface* 2:129–130. <https://doi.org/10.1098/rsif.2004.0021>
- Miller EA, Singer GP, Peterson ML, Chapman ED, Johnston ME, Thomas MJ, Battleson RD, Gingras M, Klimley AP (2020) Spatio-temporal distribution of green sturgeon (*Acipenser medirostris*) and white sturgeon (*A. transmontanus*) in the San Francisco Estuary and Sacramento River, California. *Environ Biol Fishes* 103:577–603. <https://doi.org/10.1007/s10641-020-00972-x>
- Mora EA, Lindley ST, Erickson DL, Klimley AP (2009) Do impassable dams and flow regulation constrain the distribution of green sturgeon in the Sacramento River, California? *J Appl Ichthyol* 25:39–47. <https://doi.org/10.1111/j.1439-0426.2009.01297.x>
- Mora EA, Battleson RD, Lindley ST, Thomas MJ, Bellmer R, Zarri LJ, Klimley AP (2018) Estimating the annual spawning run size and population size of the southern distinct population segment of green sturgeon. *Trans Am Fish Soc* 147:195–203. <https://doi.org/10.1002/tafs.10009>
- Moser ML, Israel JA, Neuman M, Lindley ST, Erickson DL, McCovey BW, Klimley AP (2016) Biology and life history of green sturgeon (*Acipenser medirostris* Ayres, 1854): state of the science. *J Appl Ichthyol* 32:67–86. <https://doi.org/10.1111/jai.13238>
- Moyle P (2002) *Inland fishes of California*. University of California Press, Berkeley
- Naisbett-Jones LC, Putman NF, Stephenson JF, Ladak S, Young KA (2017) A magnetic map leads juvenile European eels to the Gulf Stream. *Curr Biol* 27:1236–1240. <https://doi.org/10.1016/j.cub.2017.03.015>
- Naisbett-Jones LC, Putman NF, Scanlan MM, Noakes DLG, Lohmann KJ (2020) Magnetoreception in fishes: the effect of magnetic pulses on orientation of juvenile Pacific salmon. *J Exp Biol*. <https://doi.org/10.1242/jeb.222091>
- National Marine Fisheries Service (NMFS) (2006) Endangered and threatened wildlife and plants: Threatened status for southern distinct population segment of North American green sturgeon. *Fed. Regist.* 71:67. pp. 17757–17766. <https://www.govinfo.gov/content/pkg/FR-2006-04-07/pdf/06-3326.pdf>. Accessed 7 April 2006
- National Marine Fisheries Service (NMFS) (2015) Southern distinct population segment of the North American green sturgeon (*Acipenser medirostris*). 5-year review: summary and evaluation. NMFS, West Coast Region, Long Beach, Calif. <https://repository.library.noaa.gov/view/noaa/17034>. Accessed 18 Mar 2018
- Newton KC, Gill AB, Kajiura SM (2019) Electroreception in marine fishes: chondrichthyans. *J Fish Biol* 95:135–154. <https://doi.org/10.1111/jfb.14068>
- Nyqvist D, Durif C, Johnsen MG, De Jong K, Forland TN, Sivle LD (2020) Electric and magnetic senses in marine animals, and potential behavioral effects of electromagnetic surveys. *Mar Environ Res* 155:104888. <https://doi.org/10.1016/j.marenvres.2020.104888>
- O’Connell CP, He P (2014) A large scale field analysis examining the effect of magnetically-treated baits and barriers on teleost and elasmobranch behavior. *Ocean Coast Manag* 96:130–137. <https://doi.org/10.1016/J.OCECOAMAN.2014.05.011>
- O’Connell CP, Abel DC, Gruber SH, Stroud EM, Rice PH (2011) Response of juvenile lemon sharks, *Negaprion brevirostris*, to a magnetic barrier simulating a beach net. *Ocean Coast Manag* 54:225–230. <https://doi.org/10.1016/J.OCECOAMAN.2010.11.006>
- Poytress WR, Gruber JJ, Van Eenennaam JP, Gard M (2015) Spatial and temporal distribution of spawning events and habitat characteristics of Sacramento River green sturgeon. *Trans Am Fish Soc* 144:1129–1142. <https://doi.org/10.1080/00028487.2015.1069213>
- Putman N (2018) Marine migrations. *Curr Biol* 28:R972–R976
- Putman NF, Scanlan MM, Billman EJ, O’Neil JP, Couture RB, Quinn TP, Lohmann KJ, Noakes DLG (2014a) An inherited magnetic map guides ocean navigation in juvenile Pacific salmon. *Curr Biol* 24:446–450. <https://doi.org/10.1016/j.cub.2014.01.017>
- Putman NF, Meinke AM, Noakes DLG (2014b) Rearing in a distorted magnetic field disrupts the ‘map sense’ of juvenile steelhead trout. *Biol Lett* 10:20140169. <https://doi.org/10.1098/rsbl.2014.0169>
- Putman NF, Williams CR, Gallagher EP, Dittman AH (2020) A sense of place: pink salmon use a magnetic map for orientation. *J Exp Biol* 223:jeb218735. <https://doi.org/10.1242/jeb.218735>
- R Core Team (2021) R: A language and environment for statistical computing. R Foundation for Statistical Computing, Vienna, Austria. <https://www.r-project.org>. Accessed 14 May 2021
- Rodgers EM, Poletto JB, Gomez Isaza DF, Van Eenennaam JP, Connon RE, Todgham AE, Seesholtz A, Heublein JC, Cech JJ, Kelly JT, Fangué NA (2019) Integrating physiological data with the conservation and management of fishes: a meta-analytical review using the threatened green sturgeon (*Acipenser medirostris*). *Conserv Physiol* 7:2019. <https://doi.org/10.1093/conphys/coz035>
- Seesholtz AM, Manuel MJ, Van Eenennaam JP (2015) First documented spawning and associated habitat conditions for green sturgeon in the Feather River, California. *Environ Biol Fishes* 98:905–912. <https://doi.org/10.1007/s10641-014-0325-9>
- Sefick SJ (2016) Stream metabolism—a package for calculating single station metabolism from diurnal Oxygen curves. R package version 1.1.2. <https://CRAN.R-project.org/package=StreamMetabolism>. Accessed 18 June 2021
- Steel AE, Thomas MJ, Klimley AP (2019) Reach specific use of spawning habitat by adult green sturgeon (*Acipenser medirostris*) under different operation schedules at Red Bluff Diversion Dam. *J Appl Ichthyol* 35:22–29. <https://doi.org/10.1111/jai.13602>
- Stoot LJ, Gibson DP, Cooke SJ, Power M (2018) Assessing the potential for using low-frequency electric deterrent barriers to reduce

- lake sturgeon (*Acipenser fulvescens*) entrainment. *Hydrobiologia* 813:223–235. <https://doi.org/10.1007/s10750-018-3533-z>
- Taormina B, Bald J, Want A, Thouzeau G, Lejart M, Desroy N, Carlier A (2018) A review of potential impacts of submarine power cables on the marine environment: knowledge gaps, recommendations and future directions. *Renew Sustain Energy Rev* 96:380–391. <https://doi.org/10.1016/J.RSER.2018.07.026>
- Tchernychev M (2013) MAGPICK—magnetic map and profile processing. User Guide. <https://geometrics.com/wp-content/uploads/2018/10/MagPick.pdf>. Accessed 23 Mar 2014
- Thomas MJ, Peterson ML, Chapman ED, Hearn AR, Singer GP, Battleson RD, Klimley AP (2014) Behavior, movements, and habitat use of adult green sturgeon, *Acipenser medirostris*, in the upper Sacramento River. *Environ Biol Fishes* 97:133–146. <https://doi.org/10.1007/s10641-013-0132-8>
- Thomas MJ, Peterson ML, Chapman ED, Fanguie NA, Klimley AP (2019) Individual habitat use and behavior of acoustically-tagged juvenile green sturgeon in the Sacramento-San Joaquin Delta. *Environ Biol Fishes* 102:1025–1037. <https://doi.org/10.1007/s10641-019-00888-1>
- Tricas TC, Carlson BA (2011) Electrorceptors and magnetoreceptors. In: Sperelakis N (ed) *Cell physiology source book*. Elsevier Inc., New York, pp 705–725
- Tricas TC, Gill A (2011) Effects of EMFs from undersea power cables on elasmobranchs and other marine species. US Dept. of the Interior, Bureau of Ocean Energy Management, Regulation, and Enforcement, Pacific OCS Region, Camarillo, CA. OCS study BOEMRE 2011-09
- Van Eenennaam JP, Linares J, Doroshov SI, Hillemeier DC, Willson TE, Nova AA (2006) Reproductive conditions of the Klamath River green sturgeon. *Trans Am Fish Soc* 135:151–163. <https://doi.org/10.1577/T05-030.1>
- Walker MM, Dennis TE, Kirschvink JL (2002) The magnetic sense and its use in long-distance navigation by animals. *Curr Opin Neurobiol* 12:735–744
- Westerberg H, Begout-Anras ML (2000) Orientation of silver eel (*Anguilla anguilla*) in a disturbed geomagnetic field. In: Moore A, Russell I (eds) *Advances in fish telemetry*. CFAS, Norwich, pp 149–375
- Westerberg H, Lagenfelt I (2008) Sub-sea power cables and the migration behaviour of the European eel. *Fish Manag Ecol* 15:369–375. <https://doi.org/10.1111/j.1365-2400.2008.00630.x>
- Wyman MT, Peter Klimley A, Battleson RD, Agosta TV, Chapman ED, Haverkamp PJ, Pagel MD, Kavet R (2018a) Behavioral responses by migrating juvenile salmonids to a subsea high-voltage DC power cable. *Mar Biol* 165:134. <https://doi.org/10.1007/s00227-018-3385-0>
- Wyman MT, Thomas MJ, McDonald RR, Hearn AR, Battleson RD, Chapman ED, Kinzel P, Minear JT, Mora EA, Nelson JM, Pagel MD, Klimley AP (2018b) Fine-scale habitat selection of green sturgeon (*Acipenser medirostris*) within three spawning locations in the Sacramento River, California. *Can J Fish Aquat Sci* 75:779–791. <https://doi.org/10.1139/cjfas-2017-0072>

Publisher's Note Springer Nature remains neutral with regard to jurisdictional claims in published maps and institutional affiliations.